RM A53C19

NACA RM A53C19

NACA

RESEARCH MEMORANDUM

EXPERIMENTAL INVESTIGATION OF THE EFFECTS OF PLAN-FORM TAPER ON THE AERODYNAMIC CHARACTERISTICS OF SYMMETRICAL UNSWEPT WINGS OF VARYING ASPECT RATIO

By Edwin C. Allen

Ames Aeronautical Laboratory
Moffett Field, Calif.

NATIONAL ADVISORY COMMITTEE
FOR AERONAUTICS

WASHINGTON

May 29, 1953

Classification cancelled (or changed to Unclassified)

By authority of NASA Tech Pub Announcement

(OFFICER AUTHORIZED TO CHANGE)

93 30 Nov 65

By .....

.....

(GRADE OF OFFICER MAKING CHANGE)

10 Apr 66

DATE

NATIONAL ADVISORY COMMITTEE FOR AERONAUTICS

RESEARCH MEMORANDUM

EXPERIMENTAL INVESTIGATION OF THE EFFECTS OF PLAN-FORM TAPER ON THE AERODYNAMIC CHARACTERISTICS OF SYMMETRICAL UNSWEPT WINGS OF VARYING ASPECT RATIO

By Edwin C. Allen

SUMMARY

An investigation was made to determine the effects of plan-form taper on the aerodynamic characteristics of a series of symmetrical, unswept wings having thicknesses of 8-percent chord. The wings were tested in combination with four different bodies of revolution over a Mach number range from 0.40 to 0.94 with a corresponding Reynolds number range from 2.58 million to 5.90 million. The lift, drag, and pitching-moment characteristics are presented for wings having aspect ratios of 2, 3, and 4 and taper ratios of 0.20 to 1.00.

The drag-divergence Mach number was unaffected by taper for a constant aspect ratio. The maximum lift-drag ratio increased when the taper ratio was reduced from 1.00 to either 0.50 or 0.20 for the aspect ratio 4 wings.

INTRODUCTION

A great number of data are available on the aerodynamic characteristics of tapered wings at high subsonic speeds; however, these data are difficult to correlate because of the differences in testing techniques used. It is the purpose of this investigation to provide comprehensive data on the effects of plan-form taper on the aerodynamic characteristics of a family of symmetrical, unswept wings.

Nine wings, in all, were investigated, three aspect ratio 4 wings having taper ratios of 1.00, 0.50, and 0.20; three aspect ratio 3 wings having taper ratios of 1.00, 0.60, and 0.33; and three aspect ratio 2 wings having taper ratios of 1.00, 0.71, and 0.50. The profiles of all

wings were the NACA 63A008. The wings were tested in combination with four different bodies of revolution to help differentiate between the effects of taper and wing-body interference.

NOTATION

A	aspect ratio, $\frac{b^2}{S}$
C_D	drag coefficient, $\frac{\text{drag}}{qS}$
C_{D_B}	body drag coefficient, $\frac{\text{body drag}}{qS}$
C_L	lift coefficient, $\frac{\text{lift}}{qS}$
C_m	pitching-moment coefficient, referred to 0.25 $\bar{c}$, $\frac{\text{pitching moment}}{qS\bar{c}}$
$\frac{L}{D}$	lift-drag ratio
M	Mach number
M_D	Mach number of drag divergence, Mach number at which $dC_D/dM = 0.1$
S	wing area, sq ft
V	airspeed, ft/sec
b	wing span, ft
c	local wing chord, ft
$\bar{c}$	mean aerodynamic chord, $\frac{\int_0^{b/2} c^2 dy}{\int_0^{b/2} c\, dy}$, ft
q	dynamic pressure, $\frac{1}{2}\rho V^2$, lb/sq ft
y	spanwise distance from plane of symmetry, ft
α	angle of attack of wing reference plane, deg

[redacted]

λ taper ratio

ρ air density, slugs per cubic foot

ΔC_D C_D minus minimum C_D

$\frac{dC_L}{d\alpha}$ lift-curve slope, per deg

$\frac{dC_m}{dC_L}$ pitching-moment-curve slope

APPARATUS AND MODELS

This investigation was conducted in the Ames 16-foot high-speed wind tunnel using 26 wing and body combinations.

Three basic aspect ratio 4 unswept wings having taper ratios of 1.00, 0.50, and 0.20 were constructed. These three wings utilized NACA 63A008 sections and all had the same areas and spans. By successively cutting off the tips, the following aspect ratios and taper ratios were obtained:

Aspect ratio	Taper ratio		
4	1.00	0.50	0.20
3	1.00	.60	.33
2	1.00	.71	.50

The wing area varied not only with aspect ratio, but also with taper ratio for the aspect ratios 3 and 2 wings.

The wings were tested in combination with four different bodies of revolution, three having a fineness ratio of 9 and one having a fineness ratio of 12, based on the length to closure.

The equations for the body contours and the principal dimensions and plan forms of the wing-body combinations are shown in figure 1.

The models were supported on a sting as shown in figure 2. The sting was of constant diameter; 3.25 inches, for a distance of 18 inches downstream from the base of the bodies, then enlarging conically to a

diameter of 5.00 inches at a distance of 40 inches downstream from the base of the bodies. The aerodynamic forces and moments were measured by means of a strain-gage balance mounted within the bodies.

TESTS AND PROCEDURE

The aerodynamic characteristics of the bodies and the wing-body combinations were investigated over a Mach number range from 0.40 to 0.94. The variation of Reynolds number with Mach number for the various wings is shown in figure 3. The angle-of-attack range was from -6° to 18° except where buffeting, tunnel power limitations, or structural strength of the model reduced the upper limit of the range.

The test data have been reduced to standard NACA coefficient form and have not been corrected for base drag. Base pressures of the four bodies were measured and are presented in coefficient form in table I. A base drag could be computed from the base areas of the bodies and the difference between the measured base pressures and the free-stream static pressure. For the aspect ratio 4 wings on the small body (fineness ratio 9), this base drag coefficient would be 0.0007 at low lift coefficients and Mach numbers up to 0.92.

Constriction corrections were applied to the tunnel-empty calibration according to the methods of reference 1. The data were corrected for tunnel-wall effects in the manner described in reference 2.

There was an interaction of the normal force and pitching moment on the chord-force component of the balance. Since this interaction did not vary systematically with lift or pitching moment and was not always consistent, no correction could be properly applied. It is believed that such a correction would not have changed any of the drag coefficients by more than ±0.0010, and its main effect would have been to decrease slightly the rate of change of drag coefficient with lift coefficient.

RESULTS AND DISCUSSION

The lift, drag, and pitching-moment characteristics of the wing-body combinations are presented in figures 4 through 13.

The variation of drag coefficient with Mach number, measured at zero lift, is shown in figure 14. The Mach numbers of drag divergence at zero lift (Mach numbers at which $dC_D/dM = 0.1$) for the wings in

combination with the body having a fineness ratio of 12 are tabulated below:

Aspect ratio	Taper ratio	M_D
4	1.00	0.85
4	.50	.85
4	.20	.85
3	1.00	.86
3	.60	.86
3	.33	.86
2	1.00	.88
2	.71	.89
2	.50	.88

The drag-divergence Mach number can be seen to be essentially unchanged by taper for any one aspect ratio and was also found to be independent of the body geometry. With a reduction in aspect ratio, the Mach number of drag divergence was increased slightly.

For all the aspect ratio 4 wings, taper had little effect on the minimum drag coefficient (fig. 14) below the drag-divergence Mach number, with the exception of the wings in combination with the body having a fineness ratio of 12. No logical explanation could be found for the differences in the minimum-drag values of these combinations. Above the drag-divergence Mach number, decreasing the taper ratio caused a reduction in minimum drag coefficient. For the wings of aspect ratios 3 or 2, the apparent differences in minimum drag coefficient due to taper are mainly due to the differences in wing area relative to body size. The wing area not only varied with aspect ratio, but also varied with taper ratio for the wings of aspect ratios 3 and 2. If the body drag coefficients (fig. 15) are based on the respective wing areas and subtracted from the total drag coefficients for these wing-body combinations from figure 14, so as to give effectively the wing-plus-interference drag, it is found that the minimum drag coefficients are about the same for all taper ratios throughout the Mach number range.

Figure 16 shows the variation of the drag-due-to-lift parameter $(\Delta C_D/C_L{}^2)$ with Mach number over a lift-coefficient range from 0 to 0.45. Taper had some effect on this parameter, but these effects followed no

consistent trend. This parameter increased with decreasing aspect ratio and was independent of body shape for any one aspect ratio.

The variation of lift-curve slopes, at zero lift, with Mach number is shown in figure 17. For the aspect ratio 4 wings, the taper ratio 0.20 wing had a lower value of lift-curve slope than either the taper ratio 1.00 or 0.50 wing up through a Mach number of 0.90. The lift-curve slopes of the taper ratio 1.00 and 0.50 wings did not vary systematically with taper. The lift-curve slopes decreased with decreasing aspect ratio; however, for any one aspect ratio, body geometry had no appreciable effect on lift-curve slope.

The variation of the lift-drag ratio with lift coefficient for the aspect ratio 4 wings in combination with the small body having a fineness ratio of 9 is shown in figure 18. The wings of taper ratios 0.50 and 0.20 exhibit a higher maximum lift-drag ratio than the taper ratio 1.00 wings for all the bodies in combination with the aspect ratio 4 wings. The effect of reducing the taper ratio from 0.50 to 0.20 on the maximum lift-drag ratio was not consistent and of small magnitude. Maximum lift-drag ratios of the wings of aspect ratios 3 and 2 could not be justly compared because of the changes in wing area with taper for these aspect ratios.

Figure 19 shows the variation of the pitching-moment-curve slope with Mach number at zero lift. It should be noted that slopes are shown even for those cases in which the curves were nonlinear. At zero lift the effect of Mach number on the aerodynamic-center position was almost unchanged by variation in taper ratio for any aspect ratio, but the variation of aerodynamic-center position with Mach number was reduced by reducing the aspect ratio.

CONCLUSIONS

From the tests of several wings, in combination with four different bodies of revolution, the following conclusions can be drawn with regard to the effects of taper and aspect ratio:

1. Effects of plan-form taper

   (a) The drag-divergence Mach number is essentially unchanged for any one aspect ratio.

   (b) The lift-curve slope did not vary systematically with taper ratio.

   (c) The effect of Mach number on the pitching-moment-curve slope at zero lift is unchanged for any one aspect ratio.

(d) For the aspect ratio 4 wings the maximum lift-drag ratio increases when the taper ratio is decreased from 1.00 to either 0.50 or 0.20.

2. Effects of aspect ratio

The drag-divergence Mach number and the drag-due-to-lift parameter increase with decreasing aspect ratio; whereas, the lift-curve slope and the variation of aerodynamic-center position with Mach number decrease with decreasing aspect ratio. All these effects are consistent with trends predicted by theory.

Ames Aeronautical Laboratory
National Advisory Committee for Aeronautics
Moffett Field, Calif.

REFERENCES

1. Herriot, John G.: Blockage Corrections for Three-Dimensional-Flow Closed-Throat Wind Tunnels, with Consideration of the Effect of Compressibility. NACA Rep. 995, 1950. (Supersedes NACA RM A7B28)

2. Silverstein, Abe, and White, James A.: Wind-Tunnel Interference with Particular Reference to Off-Center Positions of the Wing, and to the Downwash at the Tail. NACA Rep. 547, 1935.

[redacted]

TABLE I.- BASE PRESSURE COEFFICIENT

M	Body of fineness ratio 12				Small body of fineness ratio 9				Large body of fineness ratio 9				Cylindrical body			
	α, deg				α, deg				α, deg				α, deg			
	0	3	6	10	0	3	6	10	0	3	6	10	0	3	6	10
0.40	0.031	0.031	0.031	0.051	-0.017	-0.017	-0.017	-0.017	0.020	0.020	0.020	0.040	-0.034	-0.034	-0.034	-0.034
.60	.031	.031	.031	.071	-.034	-.034	-.034	-.017	.026	.026	.040	.079	-.051	-.051	-.034	0
.70	.041	.041	.041	.071	-.034	-.034	-.034	-.017	.026	.026	.033	—	-.051	-.051	-.034	0
.80	.061	.061	.061	—	-.034	-.034	-.034	0	.033	.033	.033	—	-.051	-.051	-.051	—
.84	.051	.051	.061	—	-.034	-.034	-.034	0	.033	.033	.046	—	-.051	-.051	-.034	—
.86	.051	.051	.061	—	-.034	-.034	-.034	-.017	.026	.026	.046	—	-.051	-.051	-.051	—
.88	.051	.051	.051	—	-.034	-.034	-.034	-.034	.026	.026	.046	—	-.051	-.051	-.034	—
.90	.051	.061	.082	—	-.034	-.034	-.034	-.017	.040	.040	.053	—	-.068	-.068	-.034	—
.92	.041	.051	.061	—	-.034	-.034	-.034	—	.026	.026	.053	—	-.068	-.068	-.051	—
.94	.051	.051	.061	—	-.051	-.068	—	—	.225	.245	—	—	-.085	-.085	0	—

Bodies / Wings NACA 63A008 section	$r = 3.75\left[1-\left(1-\frac{2x}{l}\right)^2\right]^{\frac{3}{4}}$ l, $0.754l = 67.87$, x, r Body of fineness ratio 12	$r = 3.75\left[1-\left(1-\frac{2x}{l}\right)^2\right]^{\frac{3}{4}}$ $0.856l = 57.74$ Small body of fineness ratio 9	$r = 4.75\left[1-\left(1-\frac{2x}{l}\right)^2\right]^{\frac{3}{4}}$ $0.763l = 65.25$ Large body of fineness ratio 9	$r_1 = 3.75\left[1-\left(1-\frac{2x}{23.58}\right)^2\right]^{\frac{3}{4}}$ $r_2 = 3.75$ $r_3 = 3.75\left[1-\left(1-\frac{2x-1.74}{67.40}\right)^2\right]^{\frac{3}{4}}$ $0.846l = 57.74$, 34.57, 11.79, (1), (2), (3) Cylindrical body
$A = 4$ $\lambda = 1.00$ $S = 5.000$ sq ft $\bar{c} = 13.42$	0.50c line, 39.24	29.12	36.62	29.12
$A = 4$ $\lambda = 0.50$ $S = 5.000$ sq ft $\bar{c} = 13.91$				
$A = 4$ $\lambda = 0.20$ $S = 5.000$ sq ft $\bar{c} = 15.40$				
$A = 3$ $\lambda = 1.00$ S 3.750 sq ft $\bar{c} = 13.42$				
$A = 3$ $\lambda = 0.60$ $S = 4.267$ sq ft $\bar{c} = 14.61$				
$A = 3$ $\lambda = 0.33$ $S = 4.630$ sq ft $\bar{c} = 16.15$				
$A = 2$ $\lambda = 1.00$ $S = 2.500$ sq ft $\bar{c} = 13.42$				
$A = 2$ $\lambda = 0.71$ $S = 3.266$ sq ft $\bar{c} = 15.47$				
$A = 2$ $\lambda = 0.50$ $S = 3.906$ sq ft $\bar{c} = 17.39$				

All dimensions in inches except as noted.

NACA

Figure 1.- Wing and body combinations tested.

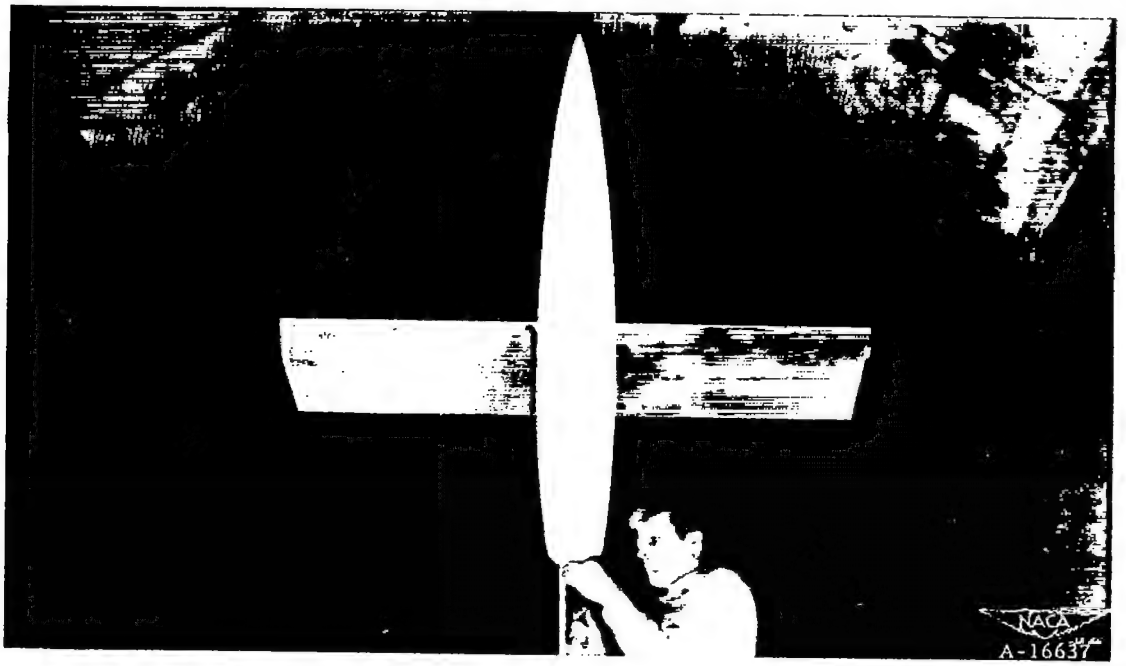

(a) Aspect ratio 4, taper ratio 1.00 wing.

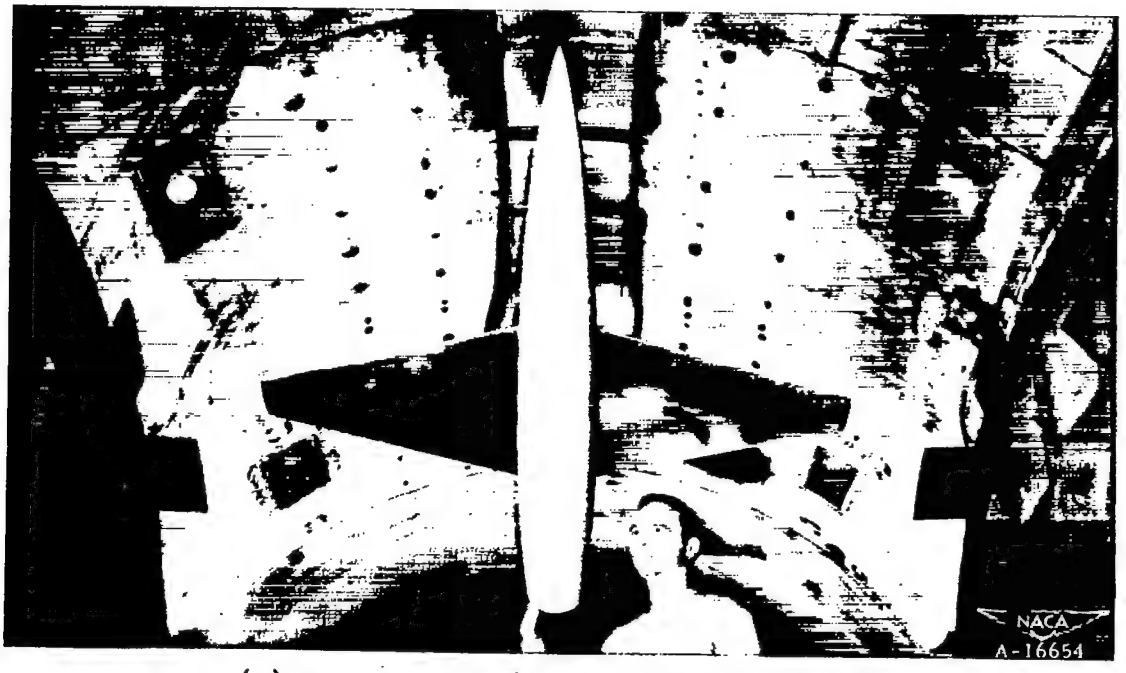

(b) Aspect ratio 4, taper ratio 0.20 wing.

Figure 2.- Two typical wings in combination with the body having a fineness ratio of 12.

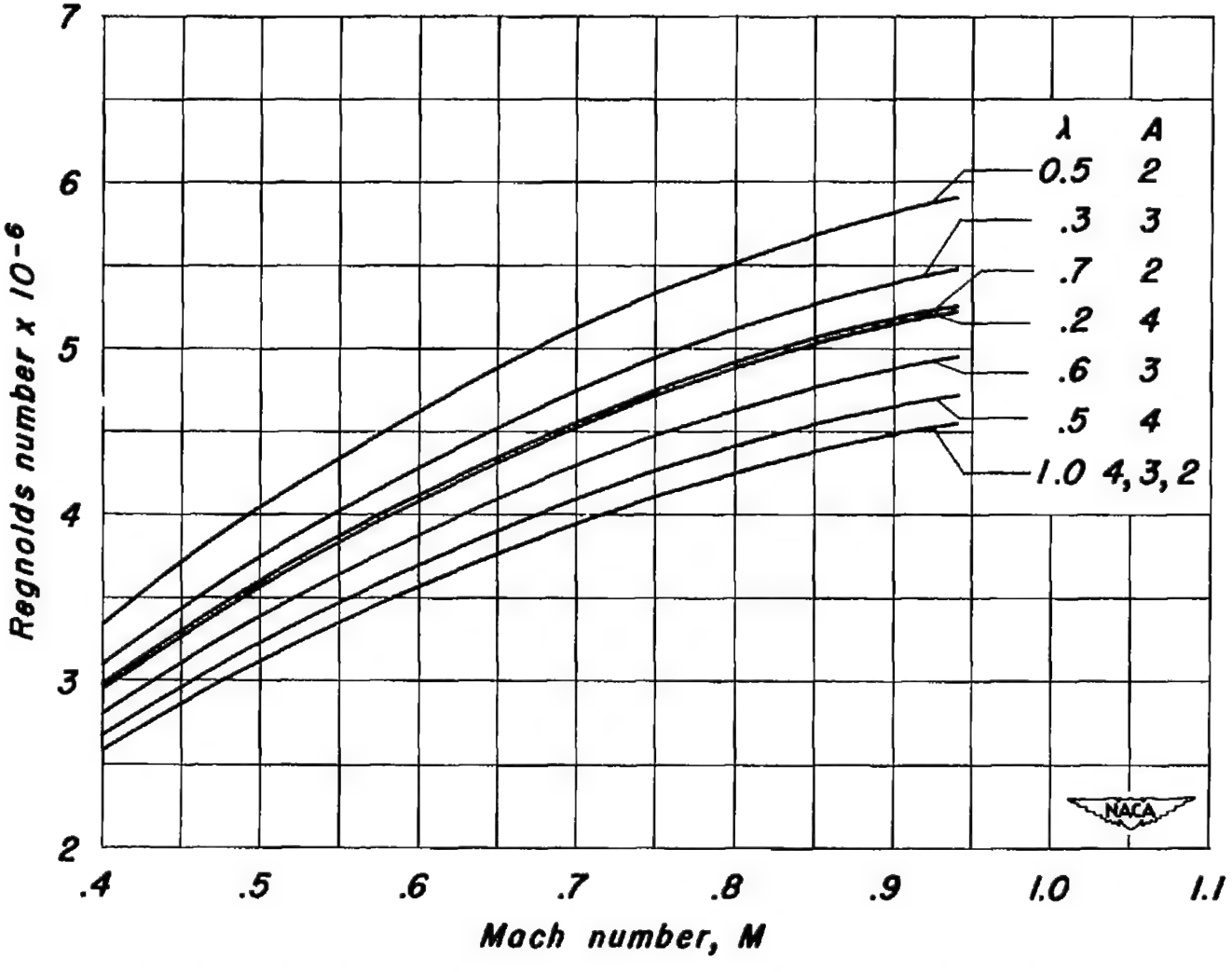

Figure 3.- The variation of test Reynolds number with Mach number.

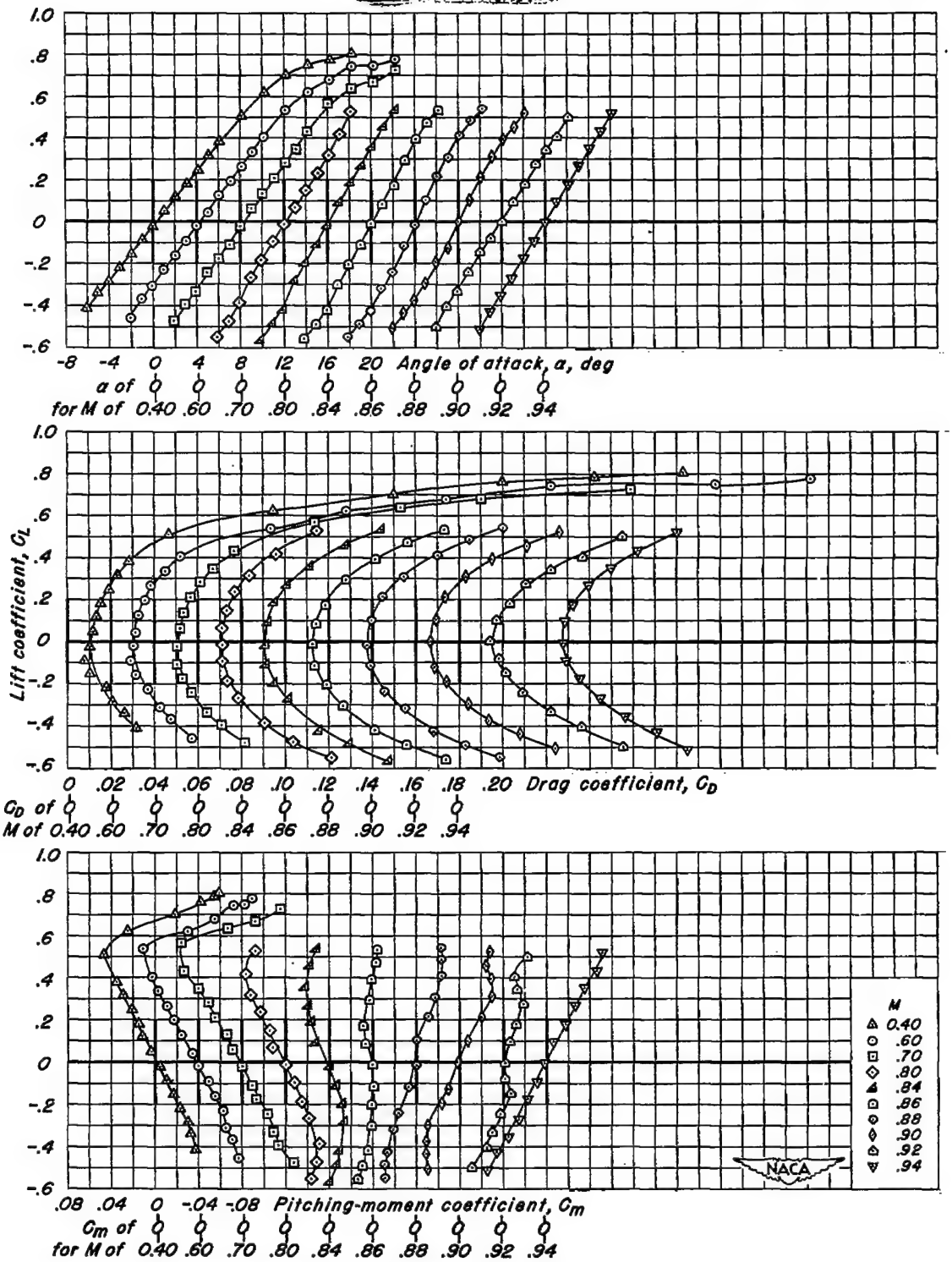

(a) Taper ratio 1.00.

Figure 4.- The lift, drag, and pitching-moment characteristics of the aspect ratio 4 wings in combination with the body having a fineness ratio of 12.

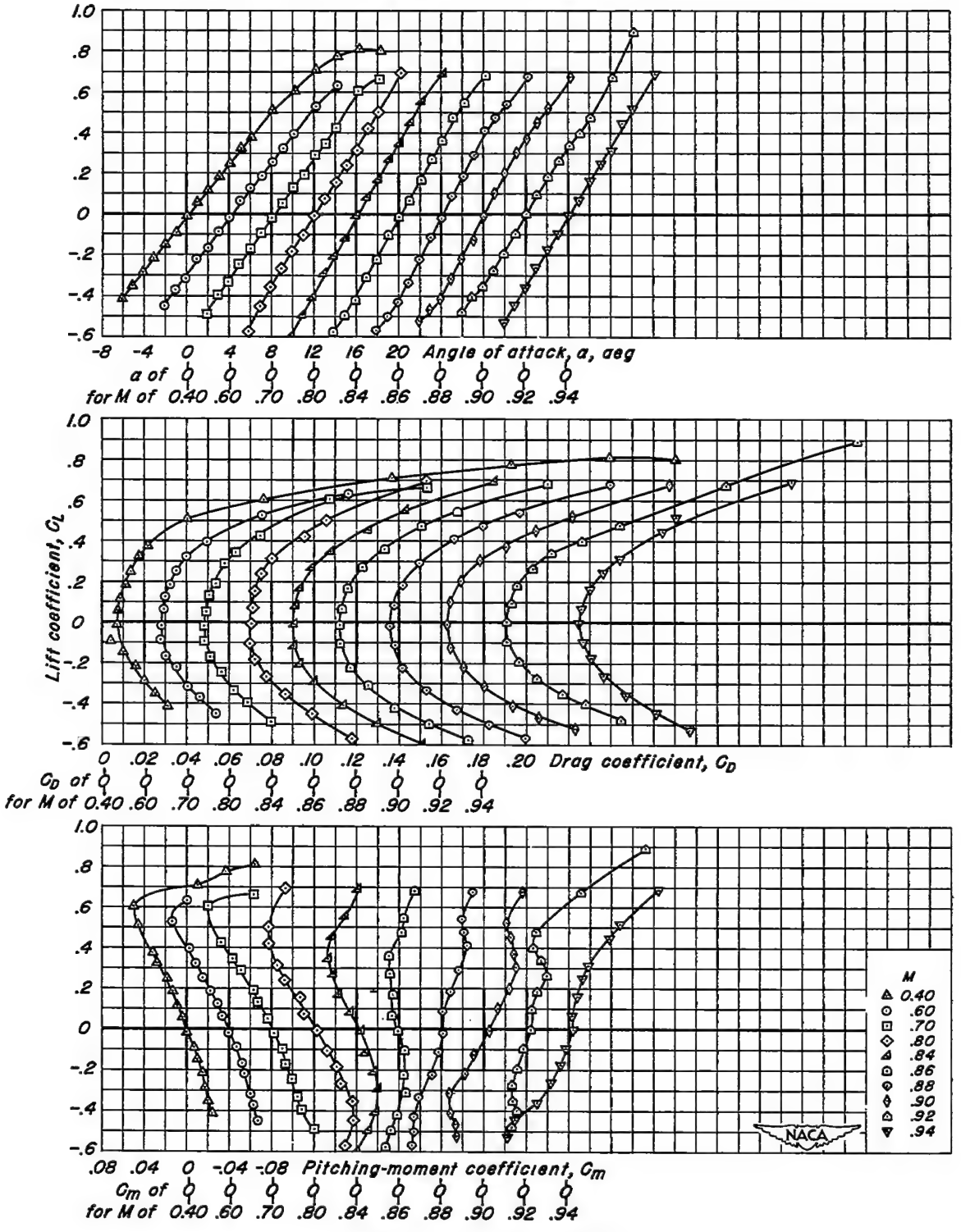

(b) Taper ratio 0.50.
Figure 4.- Continued.

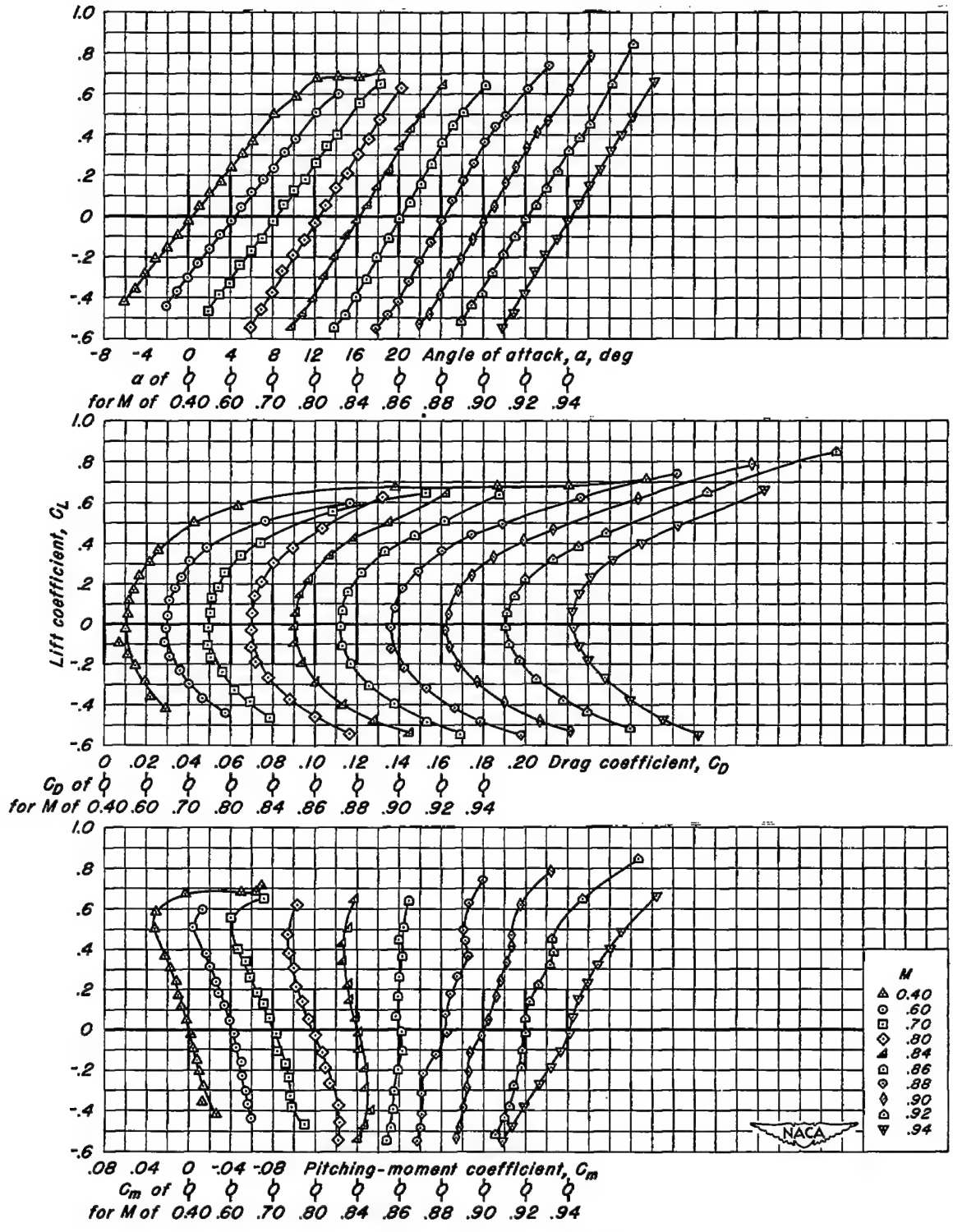

(c) Taper ratio 0.20.
Figure 4.- Concluded.

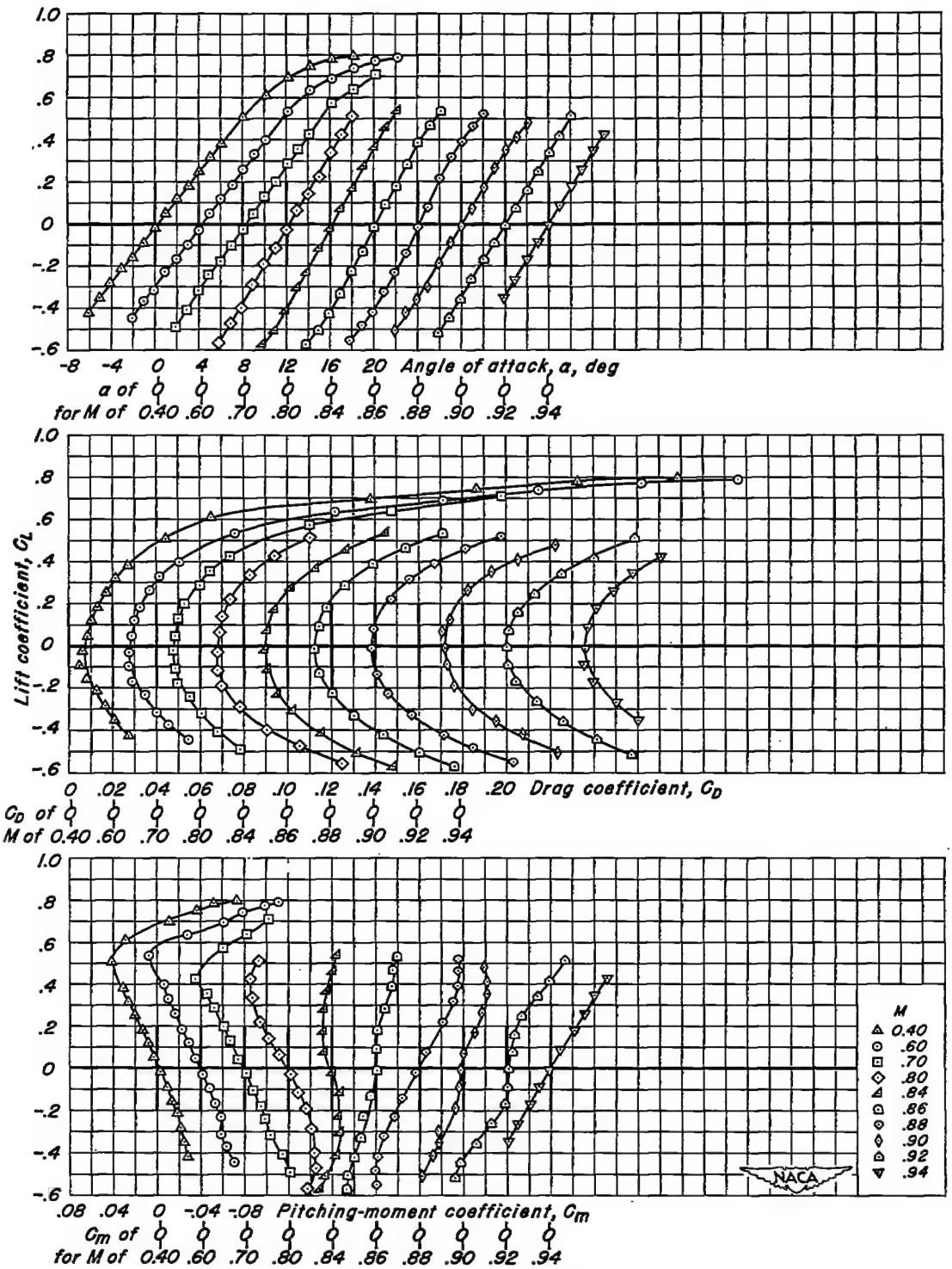

(a) Taper ratio 1.00.

Figure 5.- The lift, drag, and pitching-moment characteristics of the aspect ratio 4 wings in combination with the small body having a fineness ratio of 9.

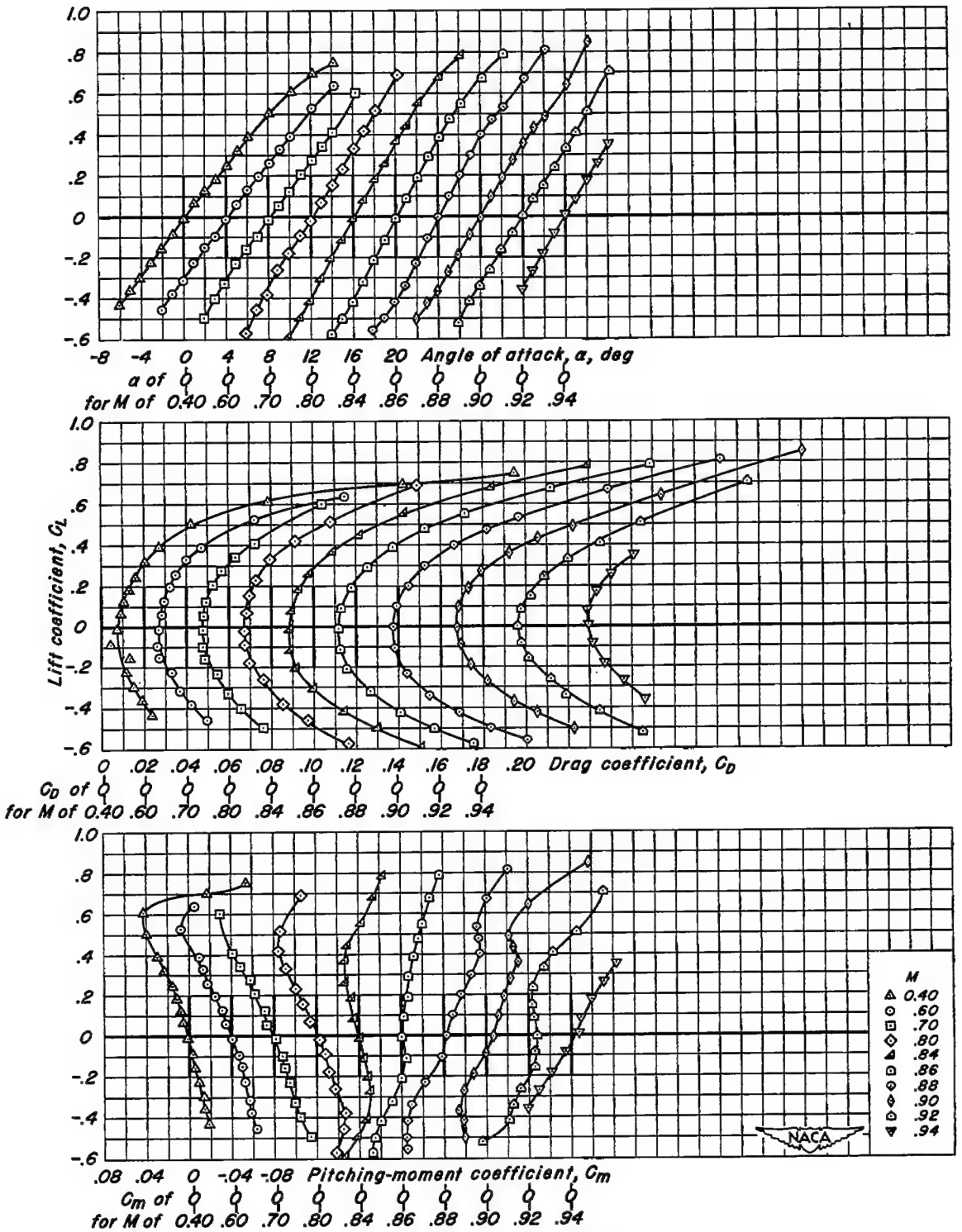

(b) Taper ratio 0.50.
Figure 5.- Continued.

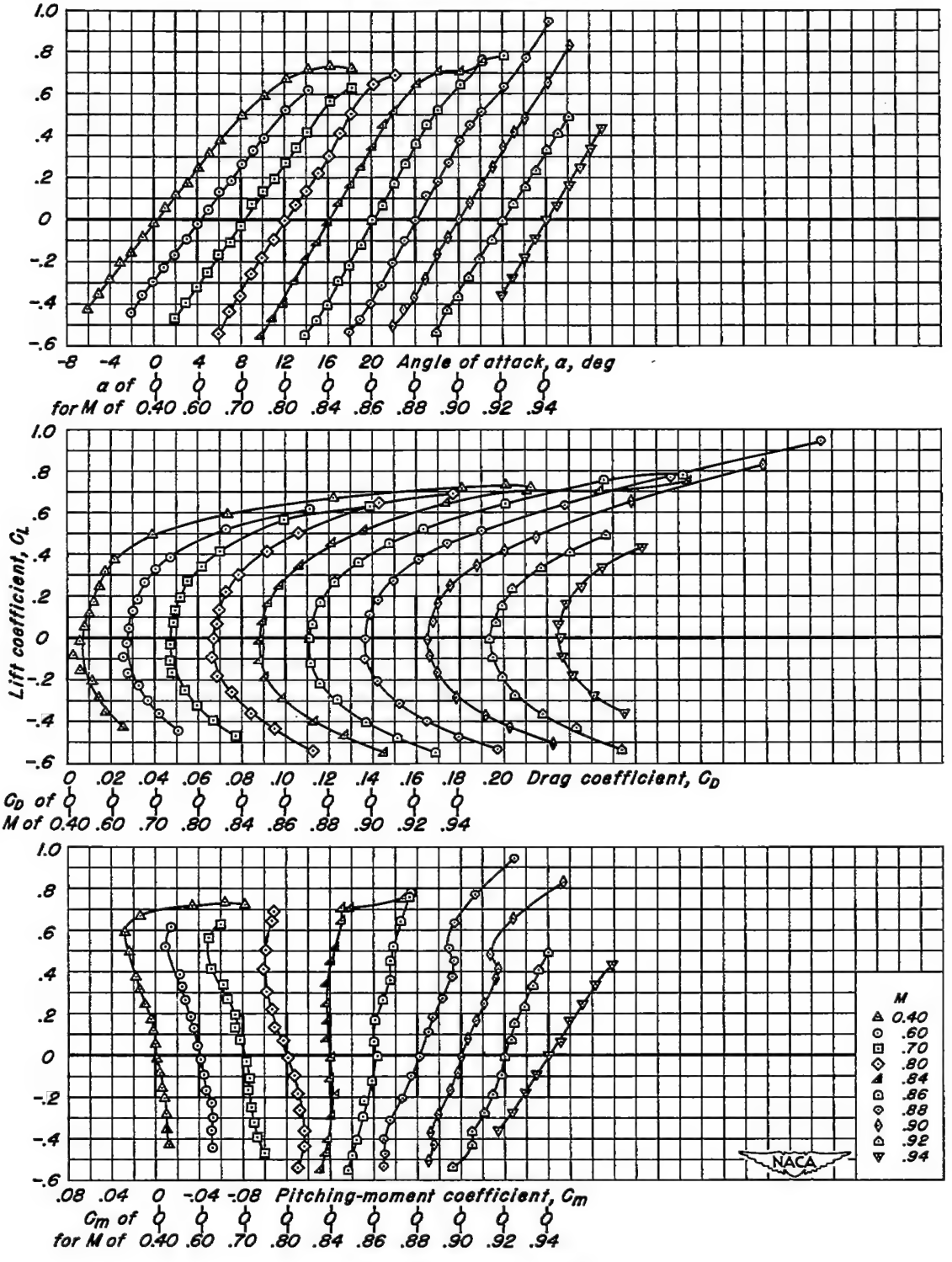

(c) Taper ratio 0.20.
Figure 5.- Concluded.

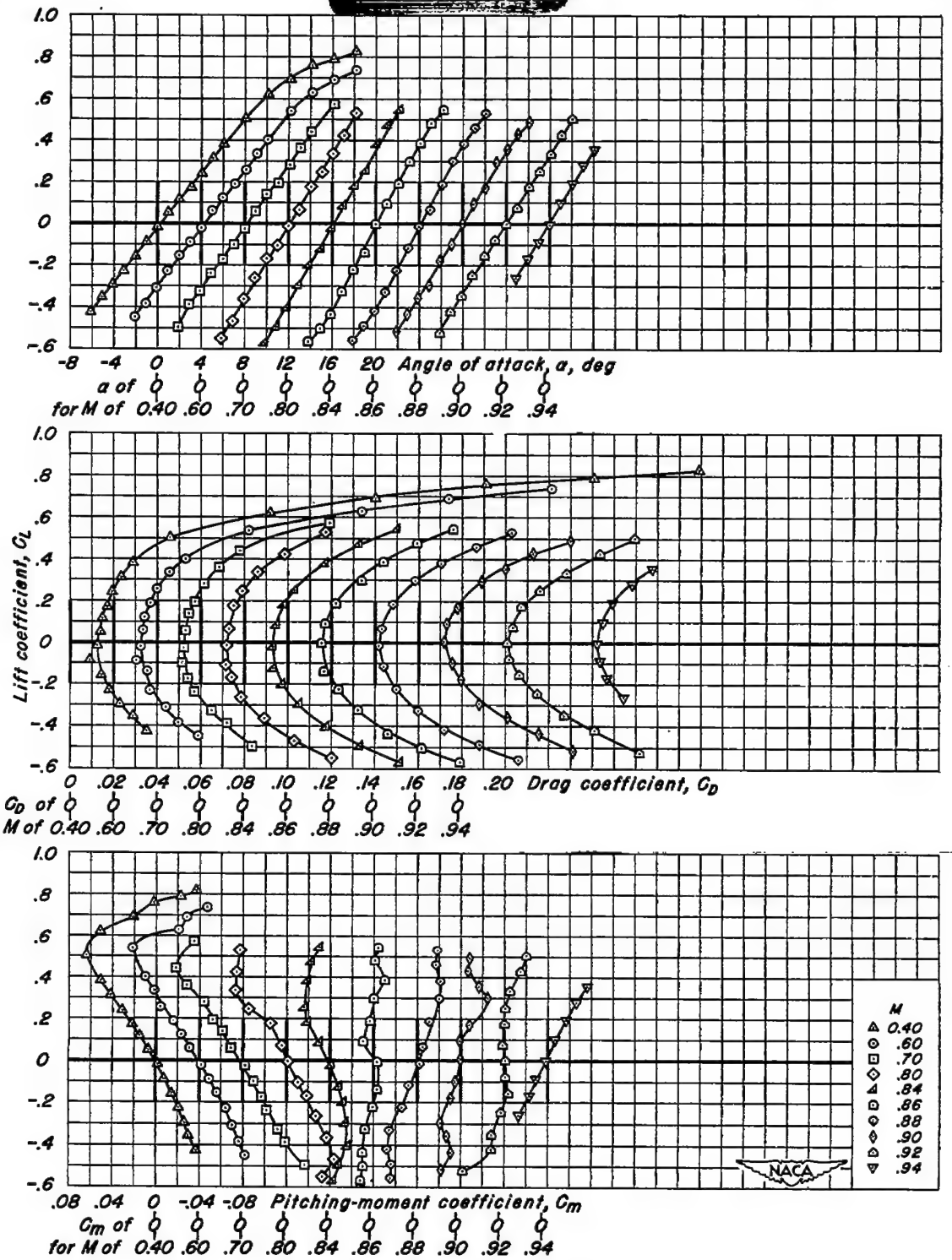

(a) Taper ratio 1.00.

Figure 6.- The lift, drag, and pitching-moment characteristics of the aspect ratio 4 wings in combination with the large body having a fineness ratio of 12.

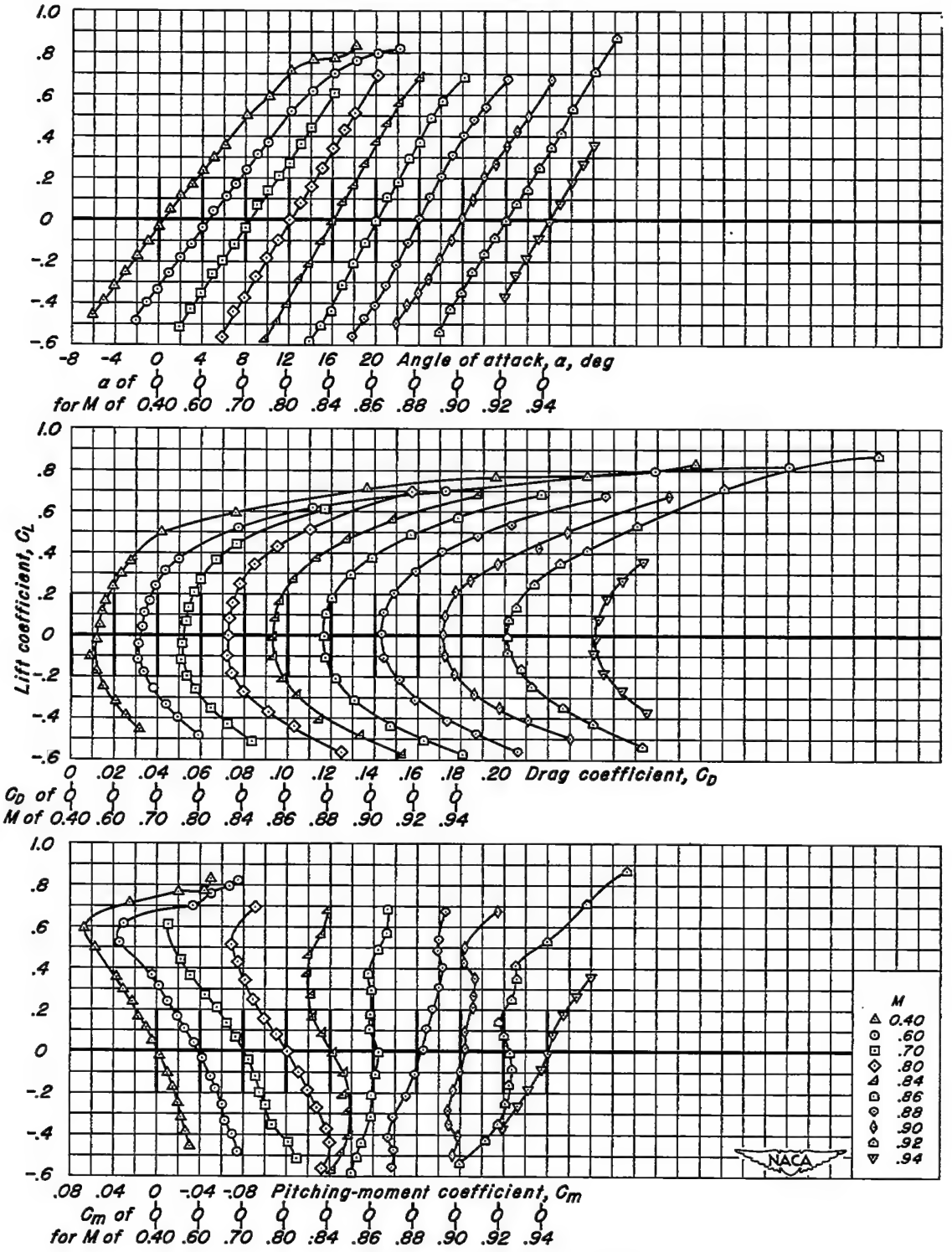

(b) Taper ratio 0.50.
Figure 6.- Continued.

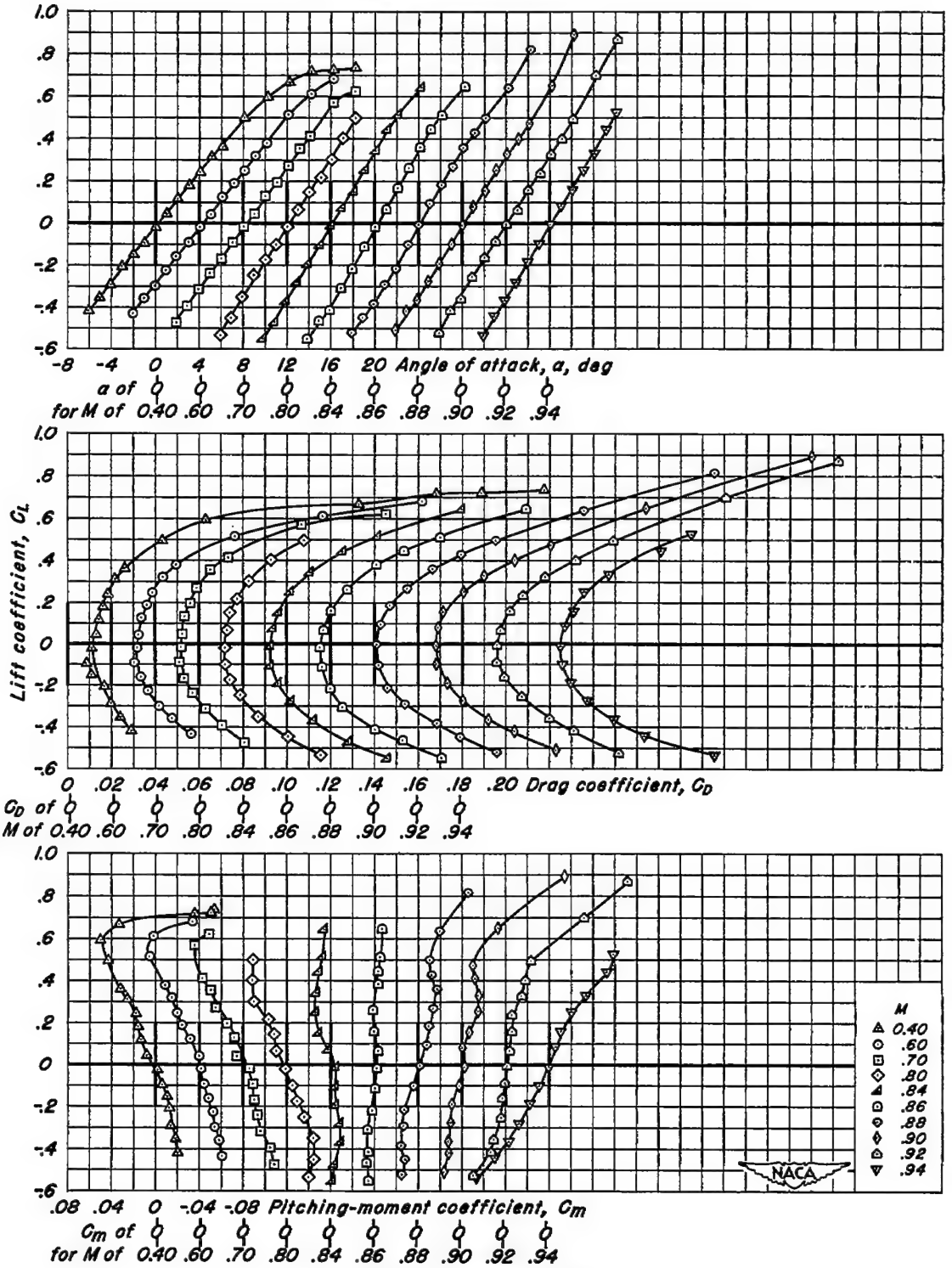

(c) Taper ratio 0.20.
Figure 6.- Concluded.

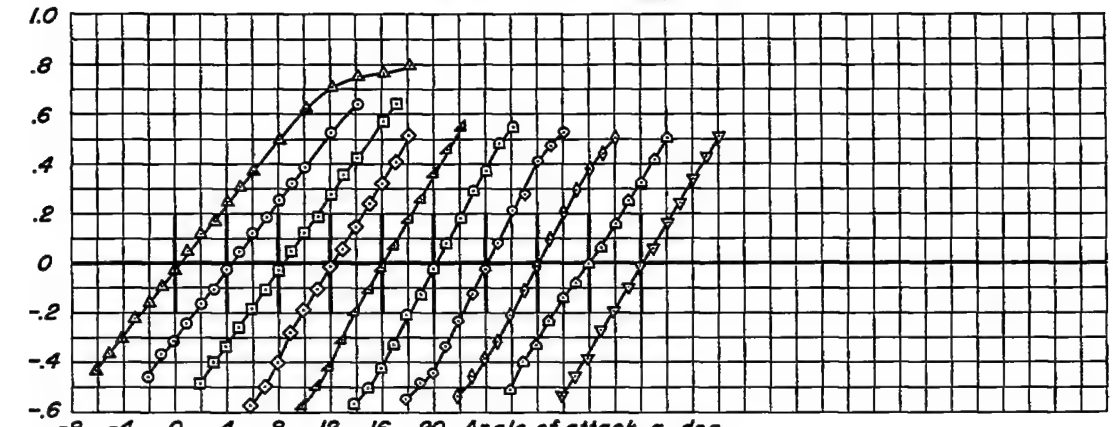

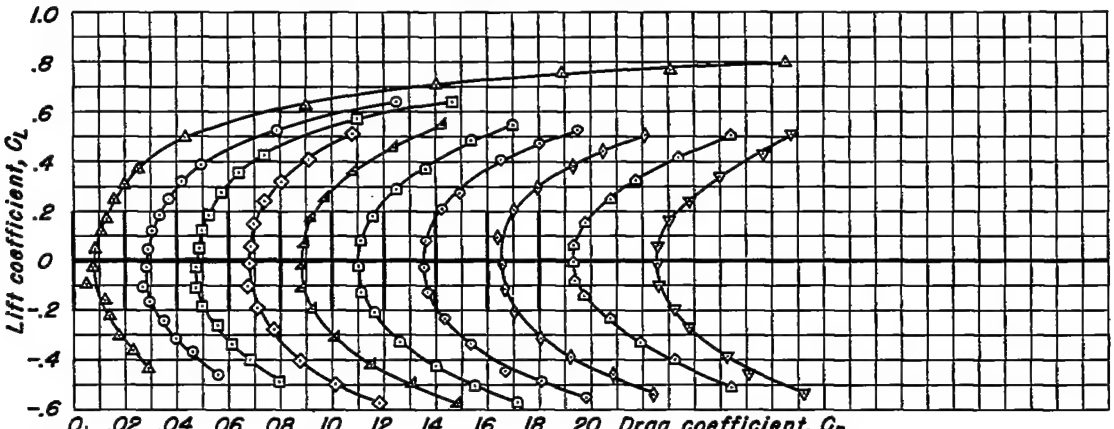

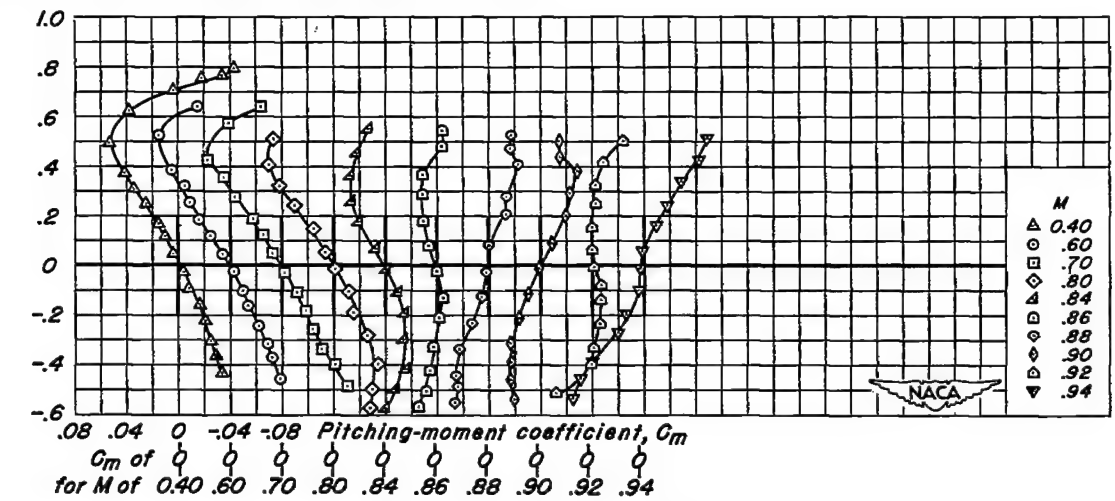

(a) Taper ratio 1.00.

Figure 7.- The lift, drag, and pitching-moment characteristics of the aspect ratio 4 wings in combination with the cylindrical body.

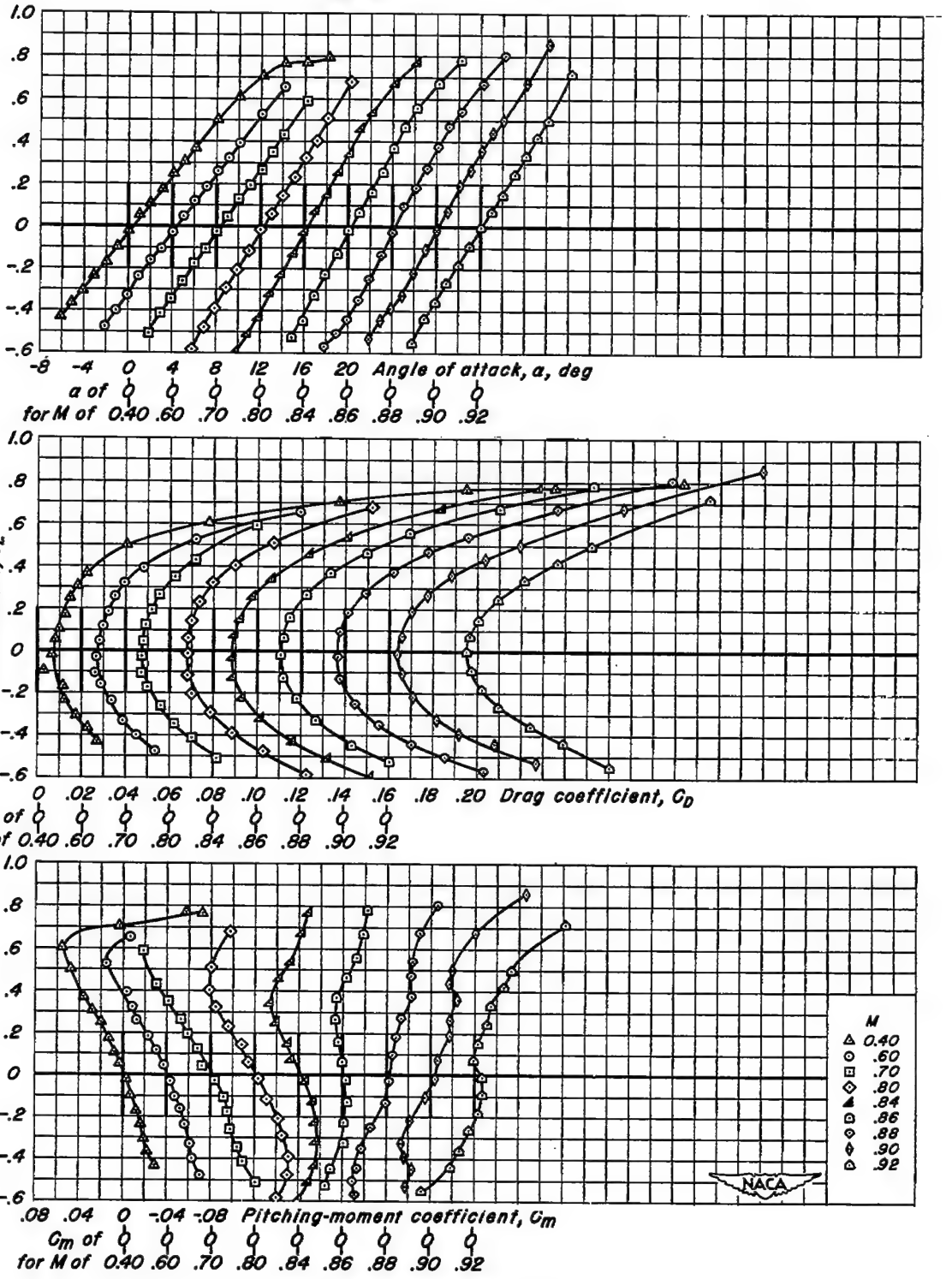

(b) Taper ratio 0.50.
Figure 7.- Continued.

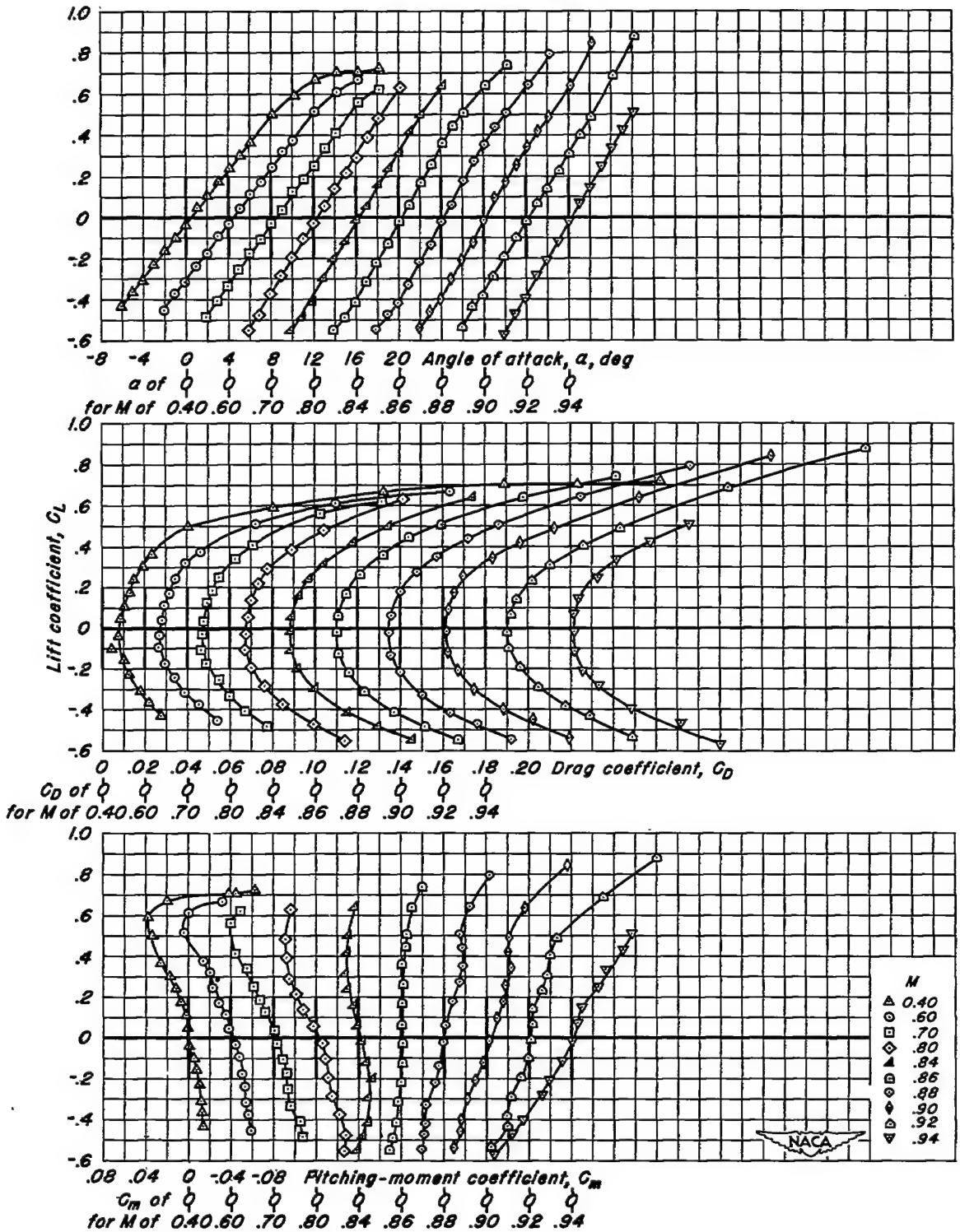

(c) Taper ratio 0.20.
Figure 7.- Concluded.

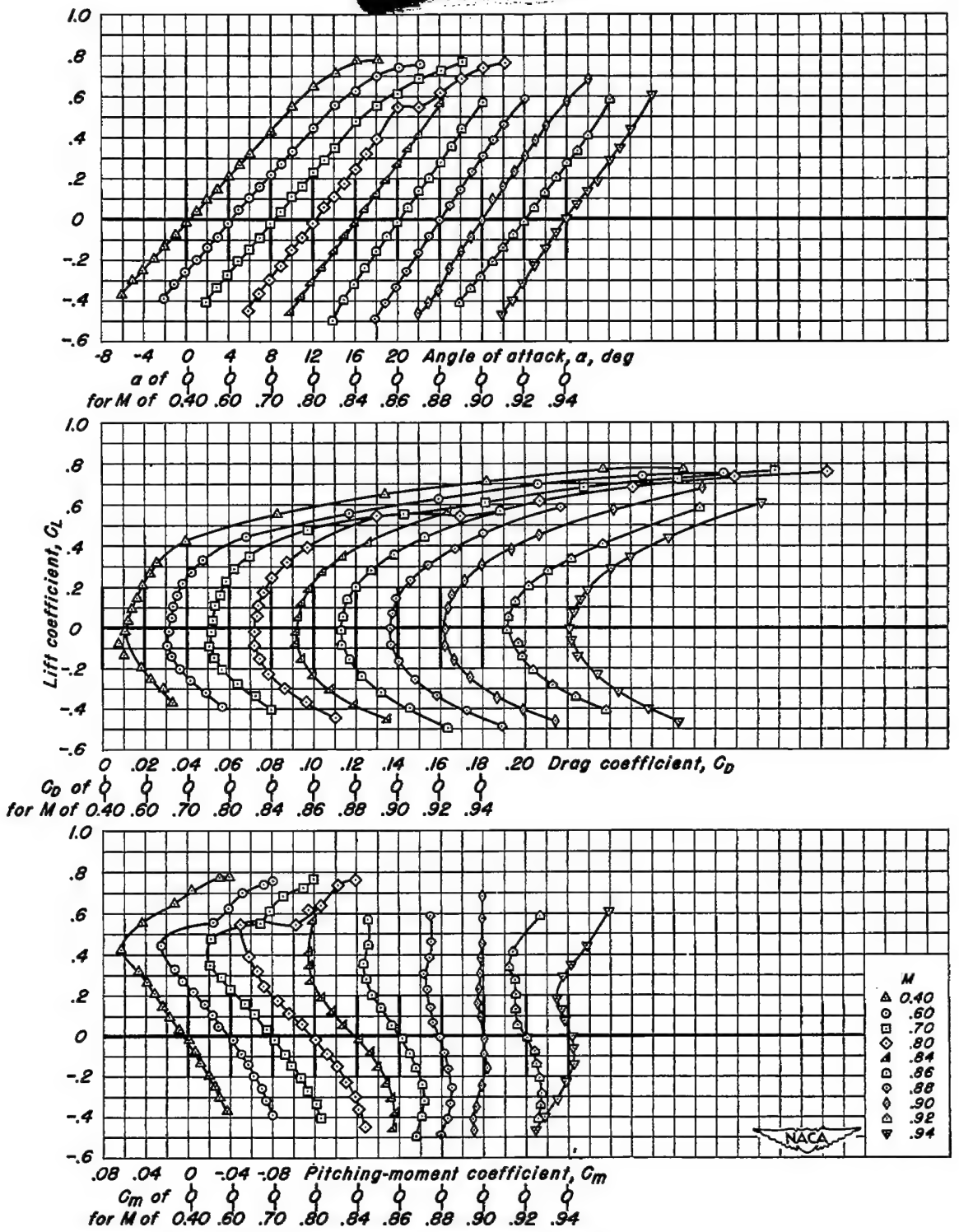

(a) Taper ratio 1.00.

Figure 8.- The lift, drag, and pitching-moment characteristics of the aspect ratio 3 wings in combination with the body having a fineness ratio of 12.

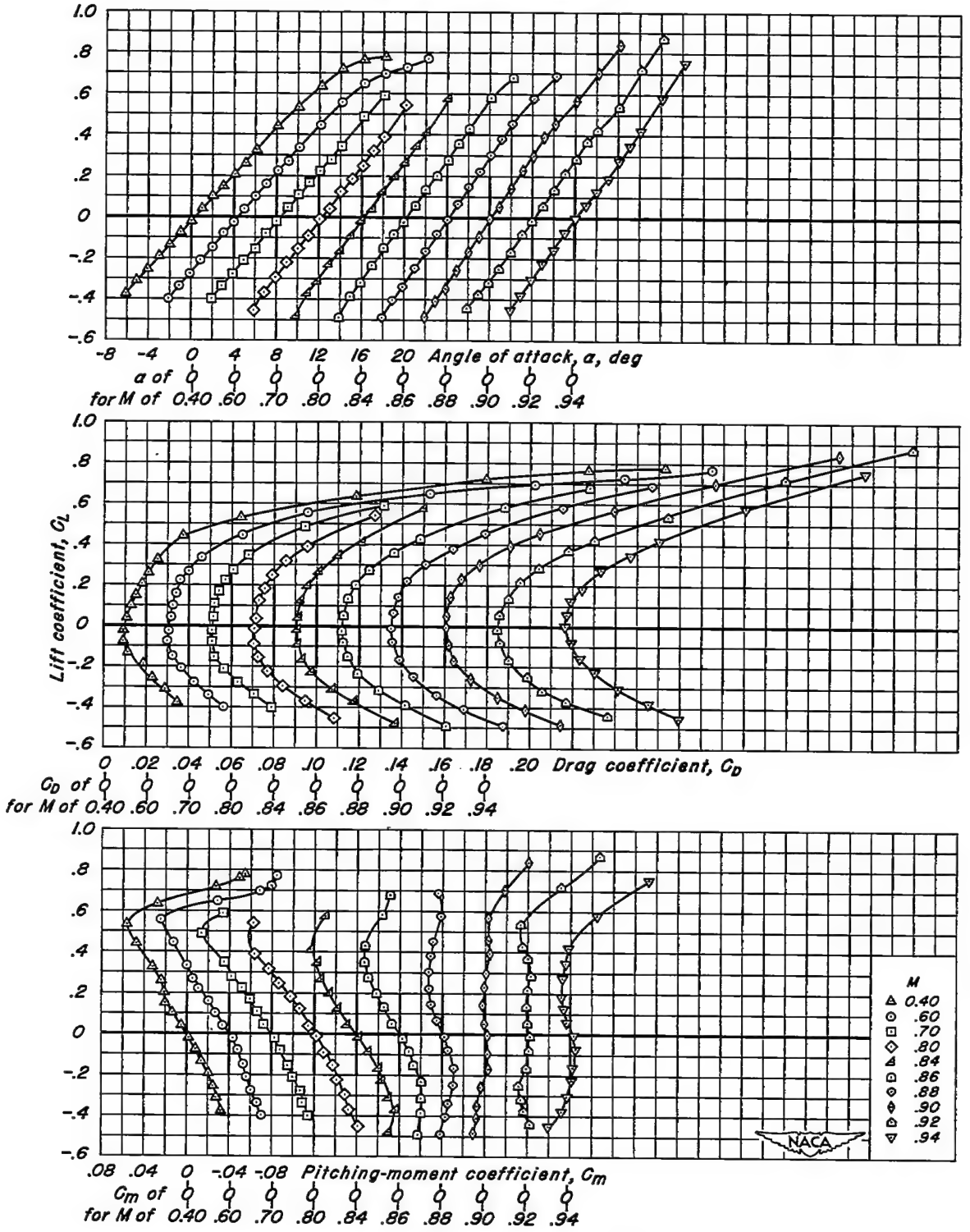

(b) Taper ratio 0.60.
Figure 8.- Continued.

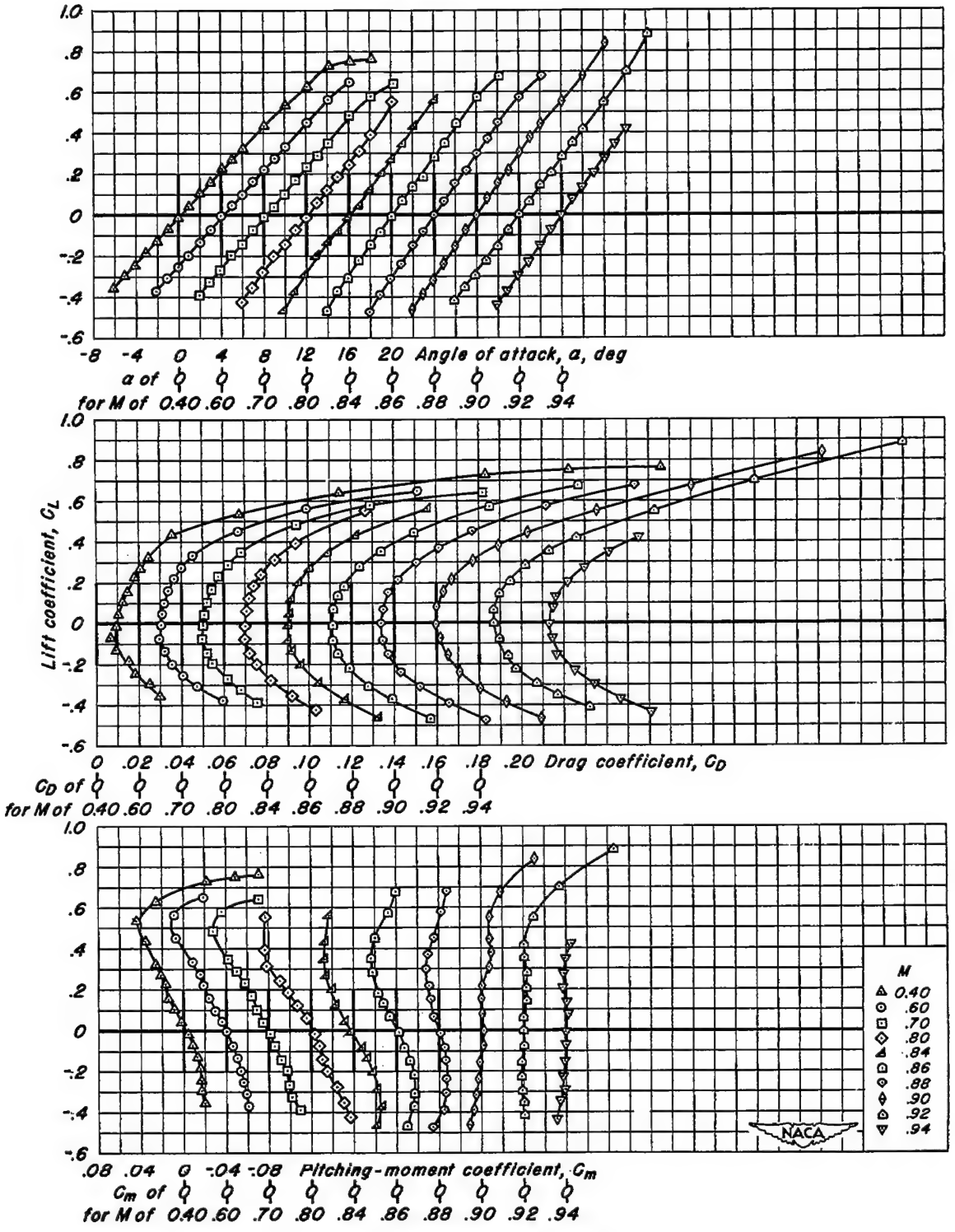

(c) Taper ratio 0.33.
Figure 8.- Concluded.

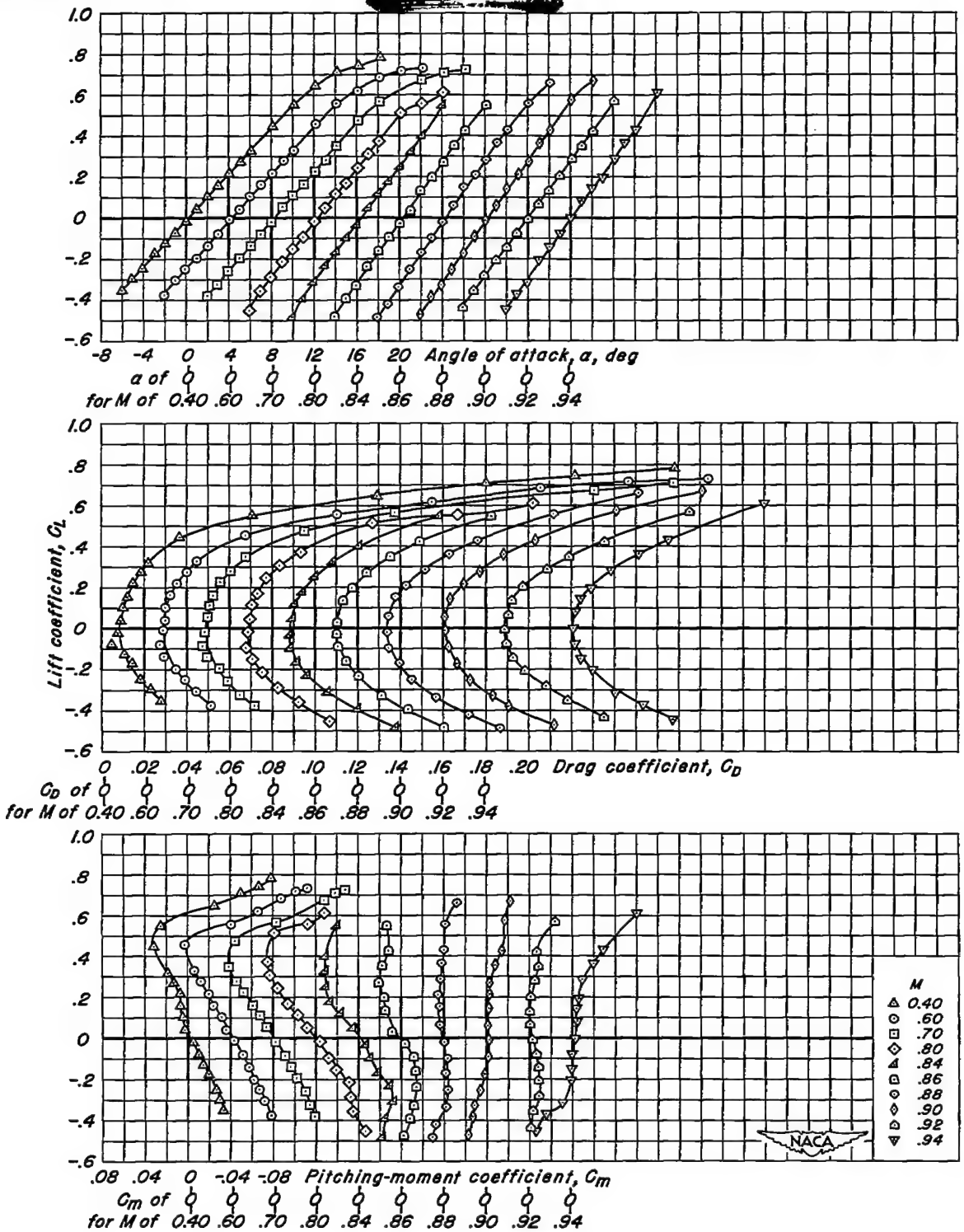

Figure 9.- The lift, drag, and pitching-moment characteristics of the aspect ratio 3, taper ratio 1.00 wing in combination with the small body having a fineness ratio of 9.

[redacted]

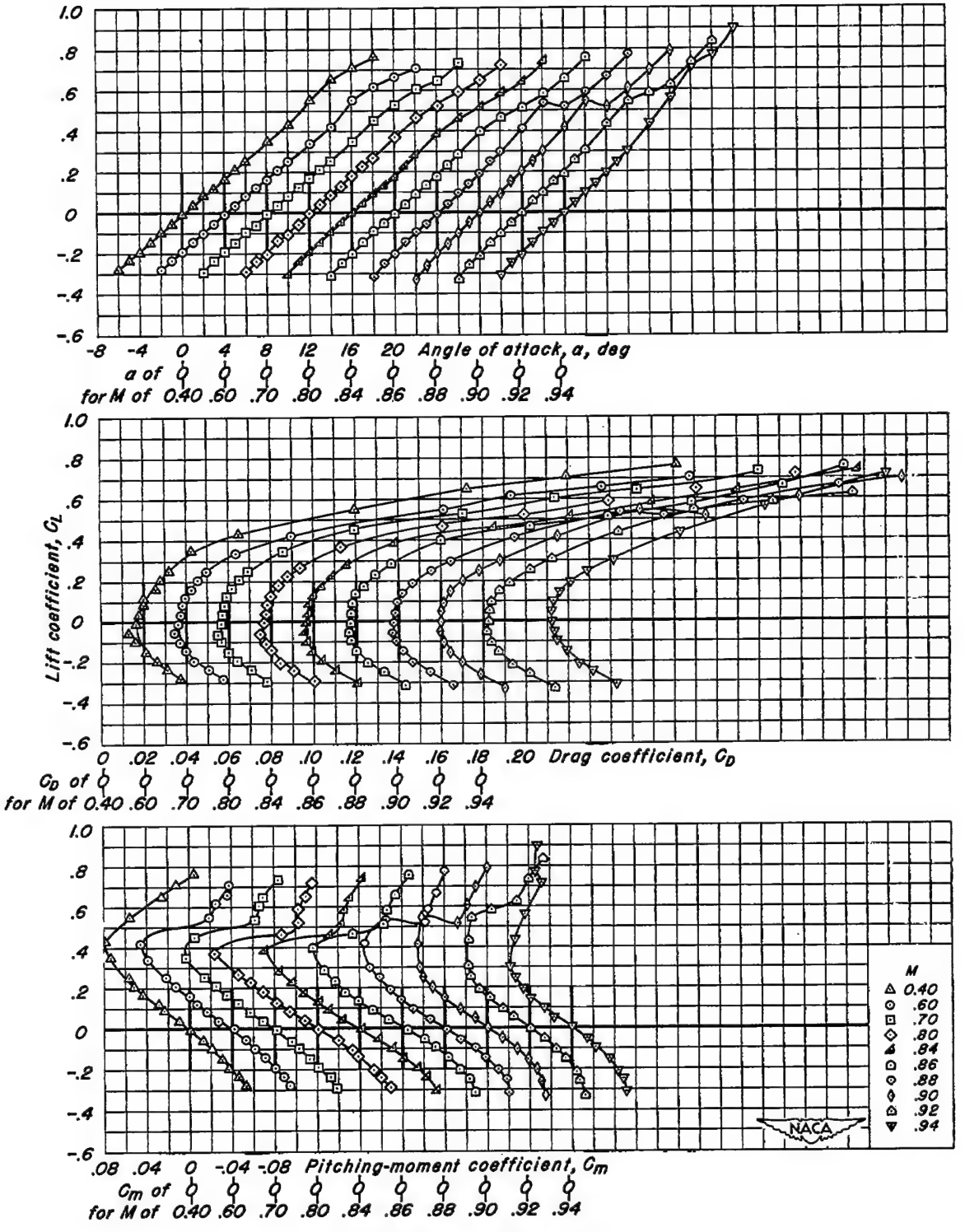

(a) Taper ratio 1.00.

Figure 10.- The lift, drag, and pitching-moment characteristics of the aspect ratio 2 wings in combination with the body having a fineness ratio of 12.

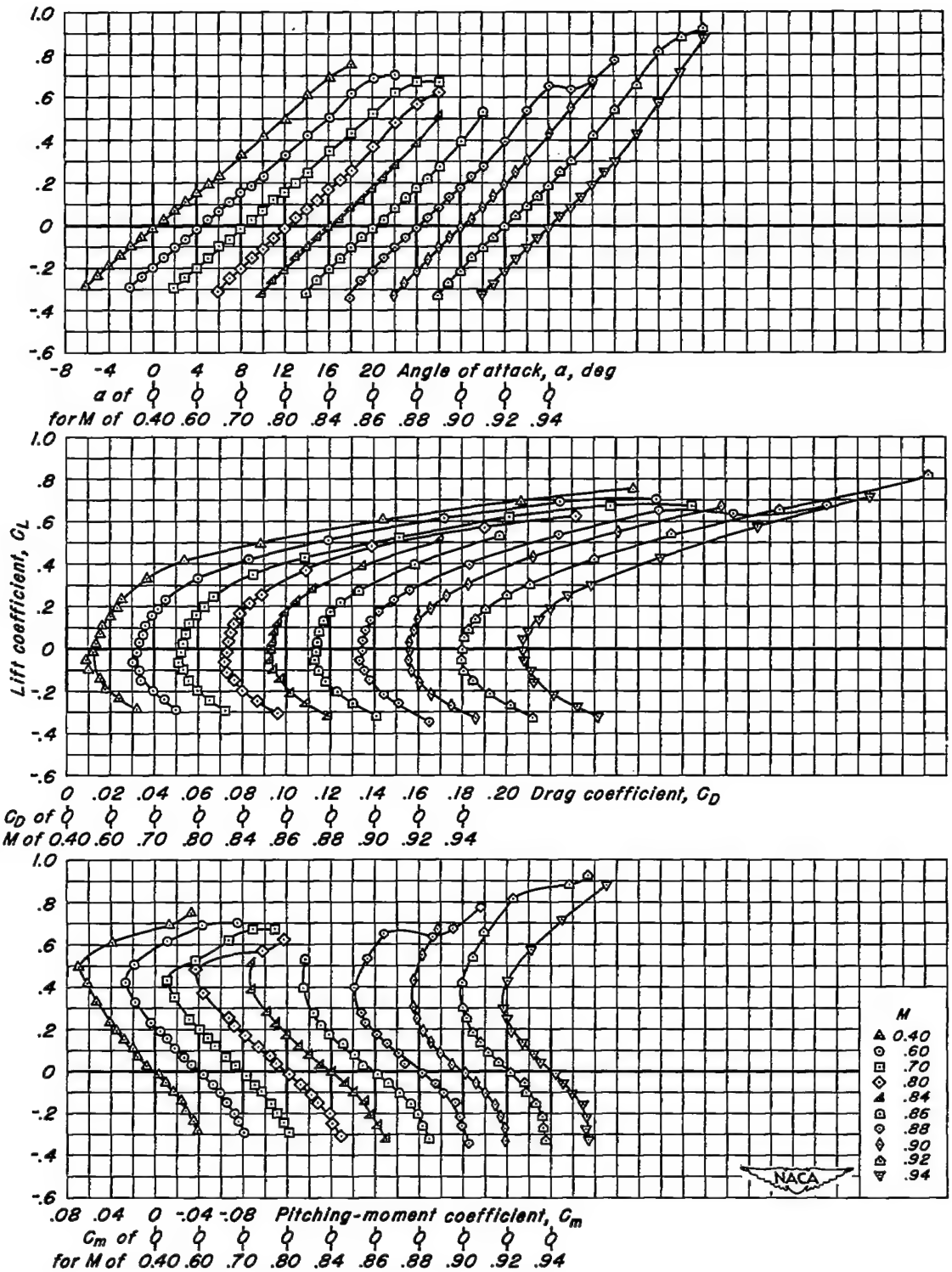

(b) Taper ratio 0.71.
Figure 10.- Continued.

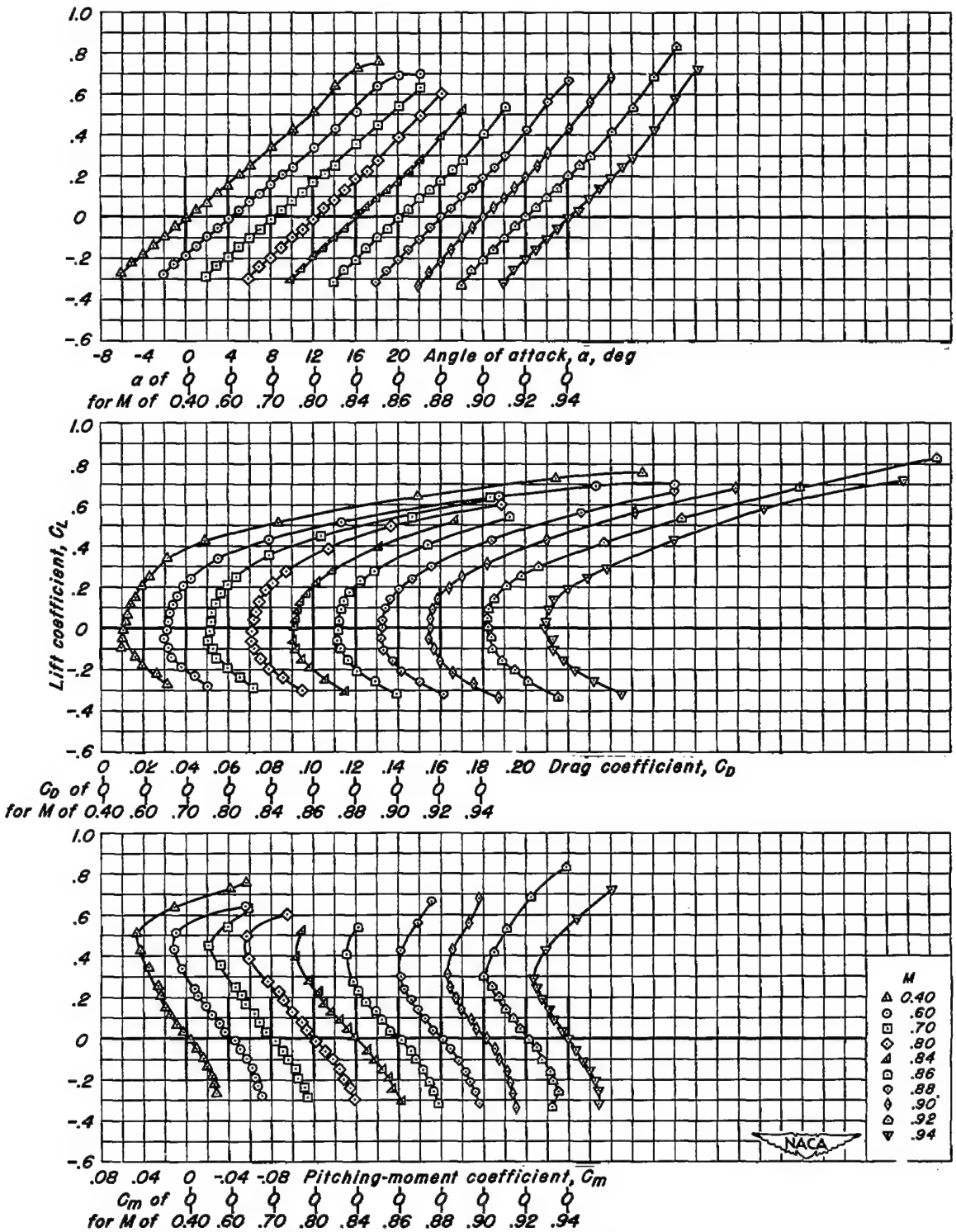

(c) Taper ratio 0.50.
Figure 10.- Concluded.

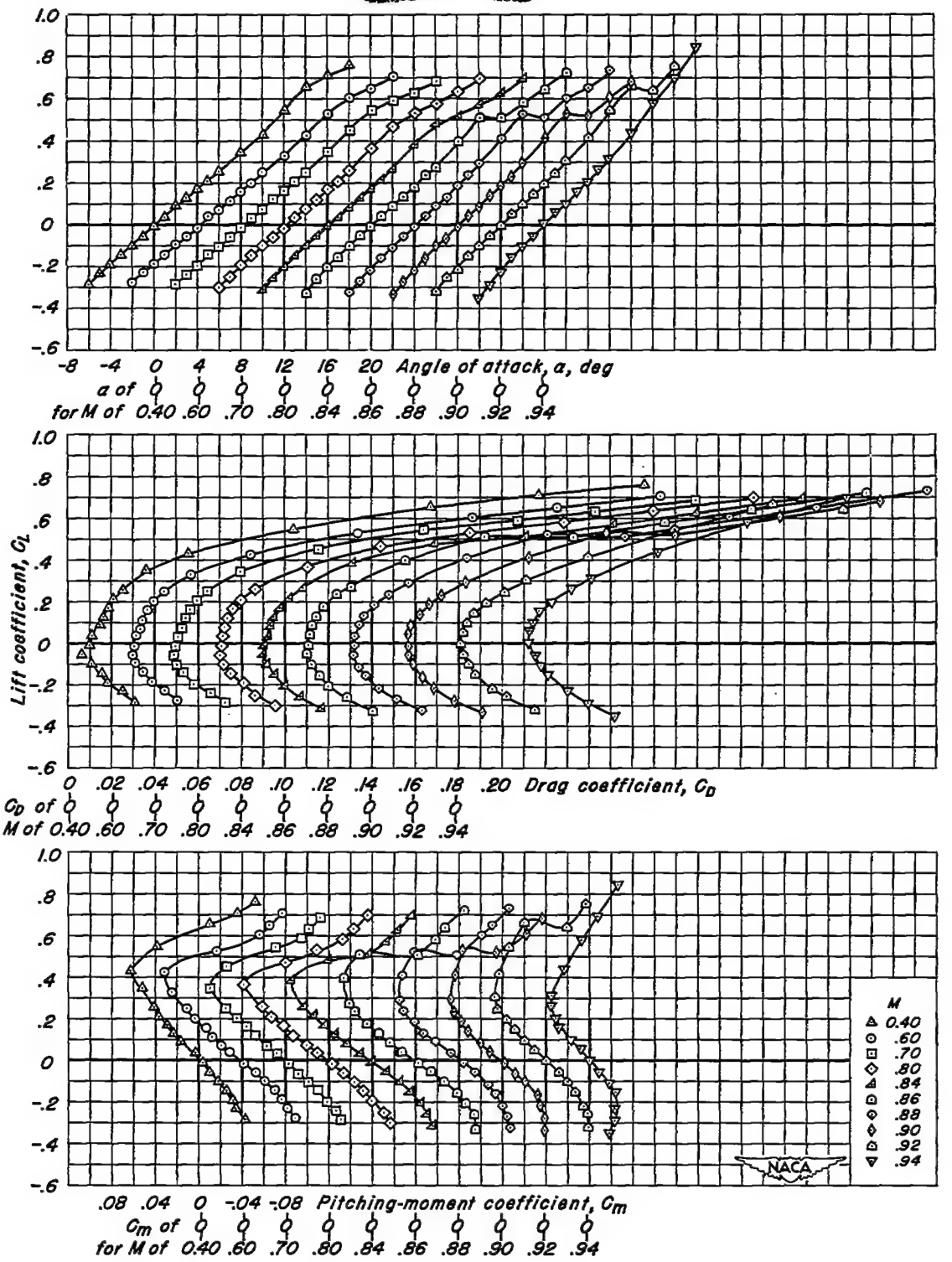

(a) Taper ratio 1.00.

Figure 11.- The lift, drag, and pitching-moment characteristics of the aspect ratio 2 wings in combination with the small body having a fineness ratio of 9.

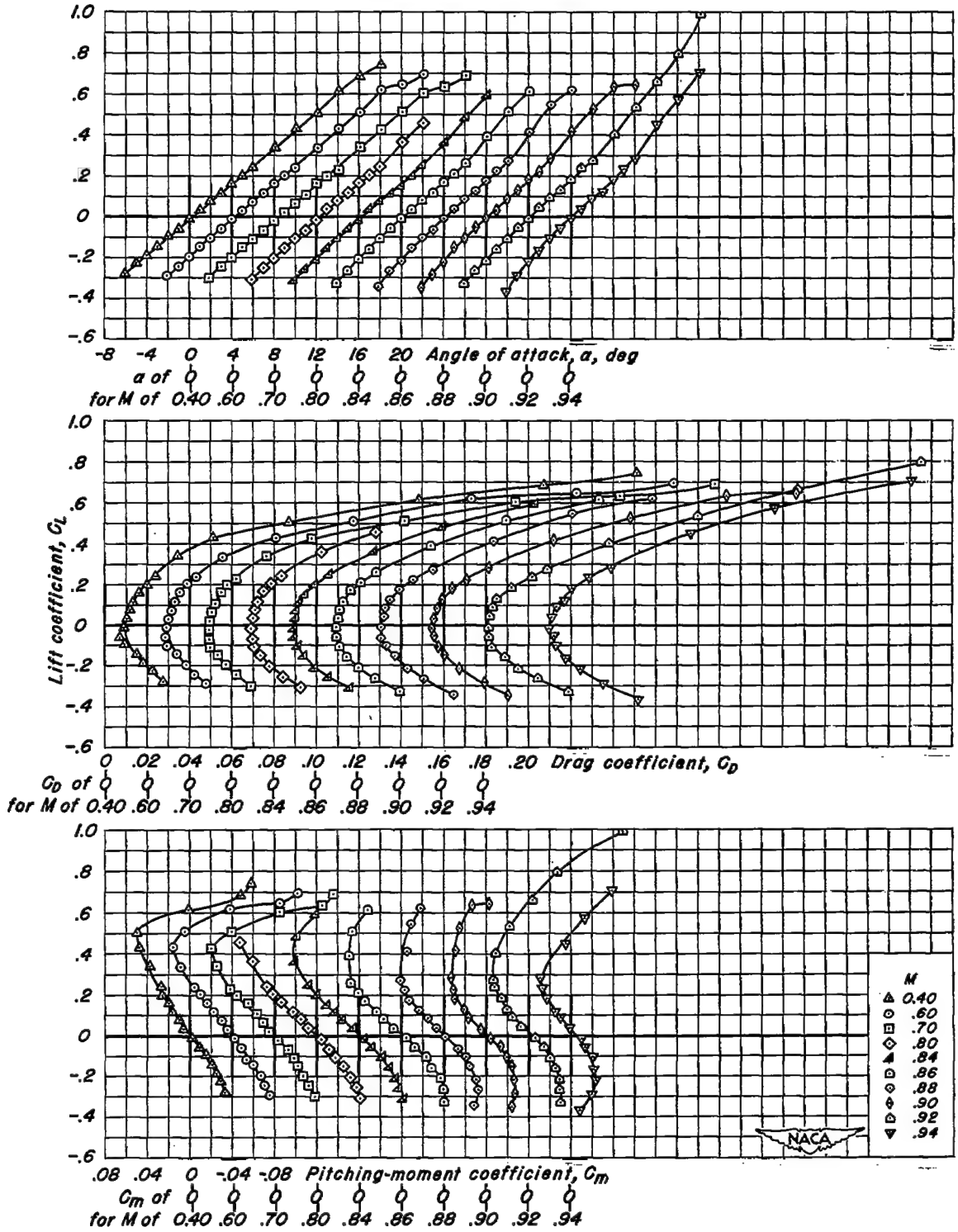

(b) Taper ratio 0.7l.
Figure 11.- Continued.

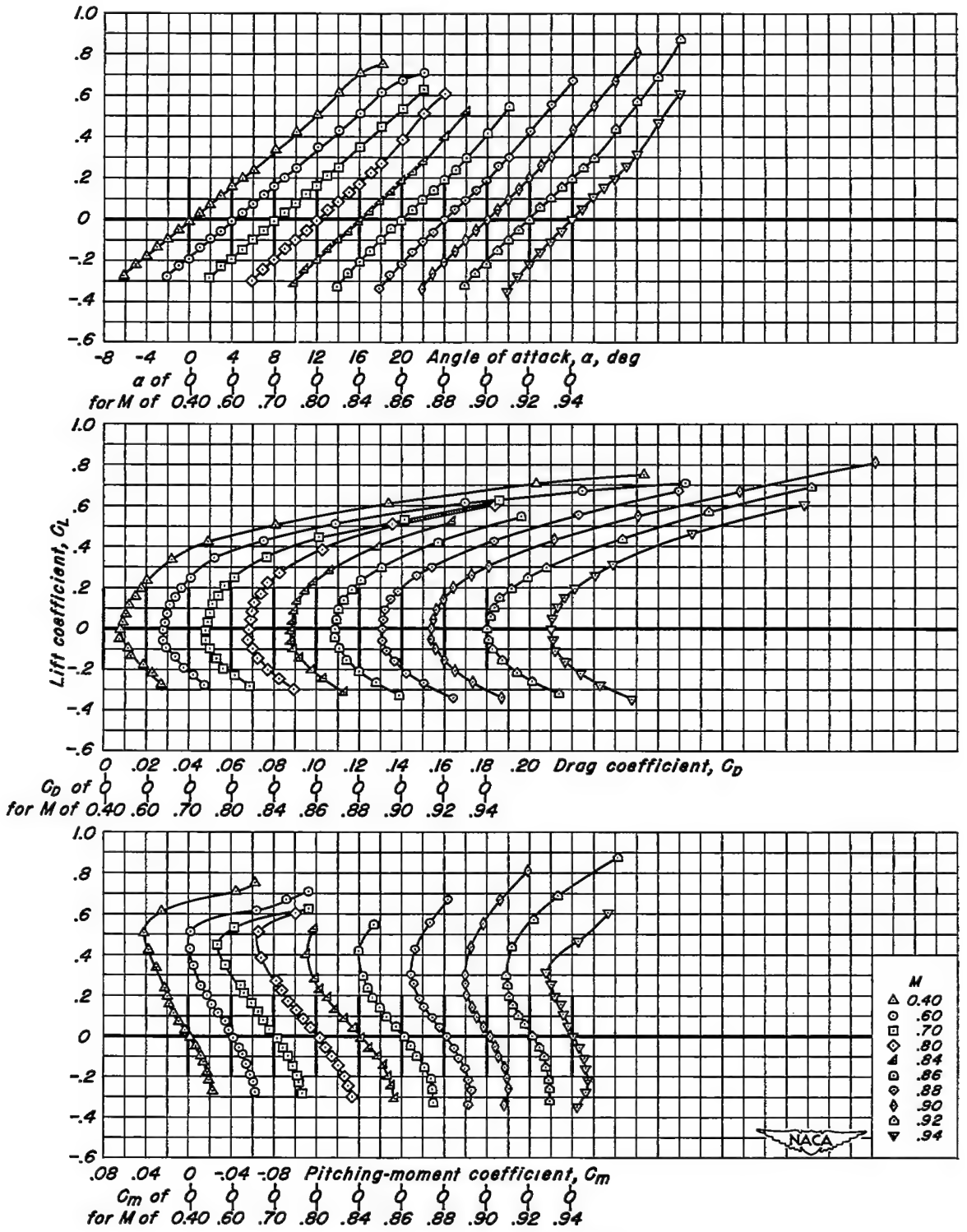

(c) Taper ratio 0.50.
Figure 11.- Concluded.

CONFIDENTIAL

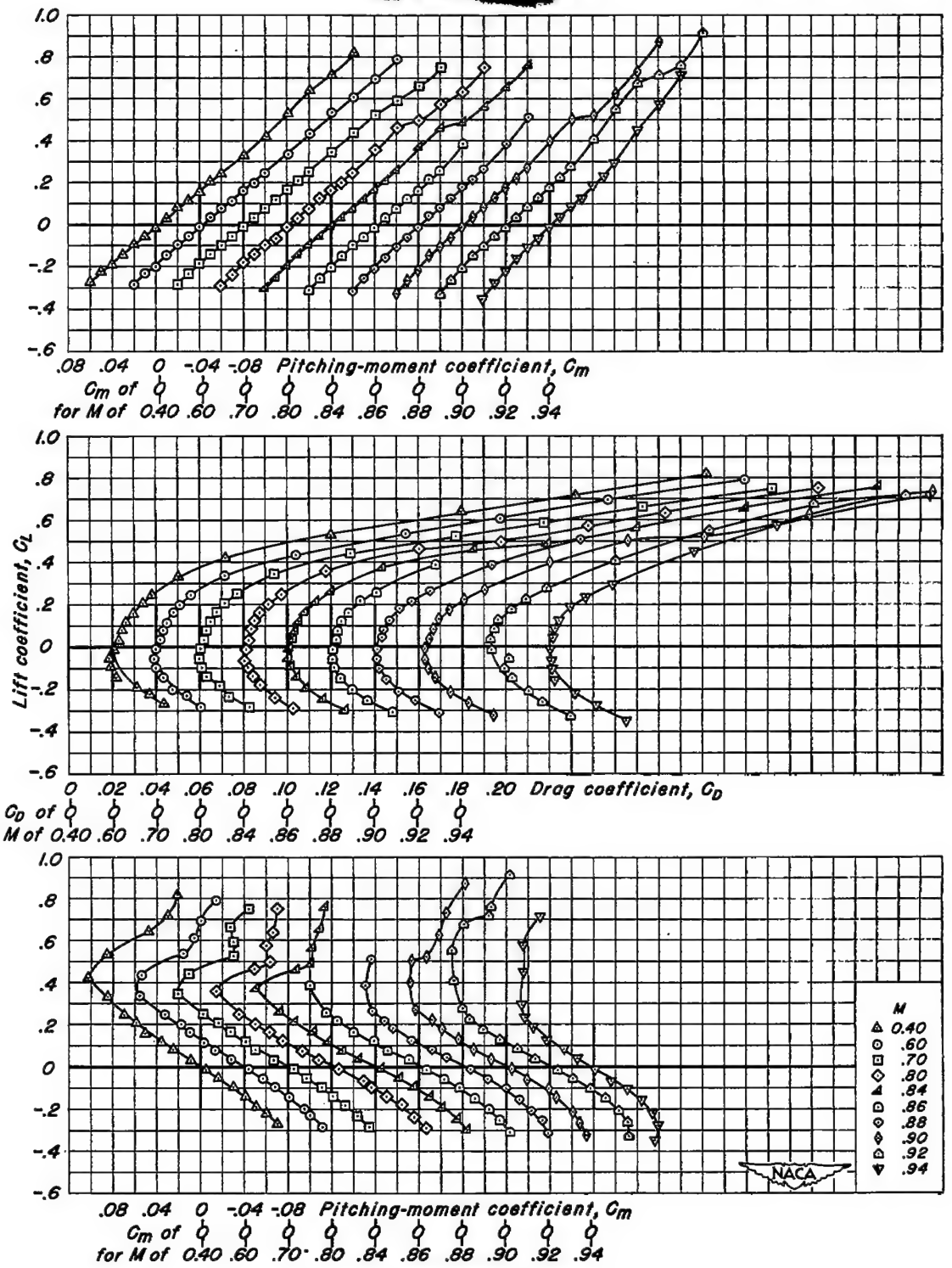

(a) Taper ratio 1.00.

Figure 12.- The lift, drag, and pitching-moment characteristics of the aspect ratio 2 wings in combination with the large body having a fineness ratio of 9.

[redacted]

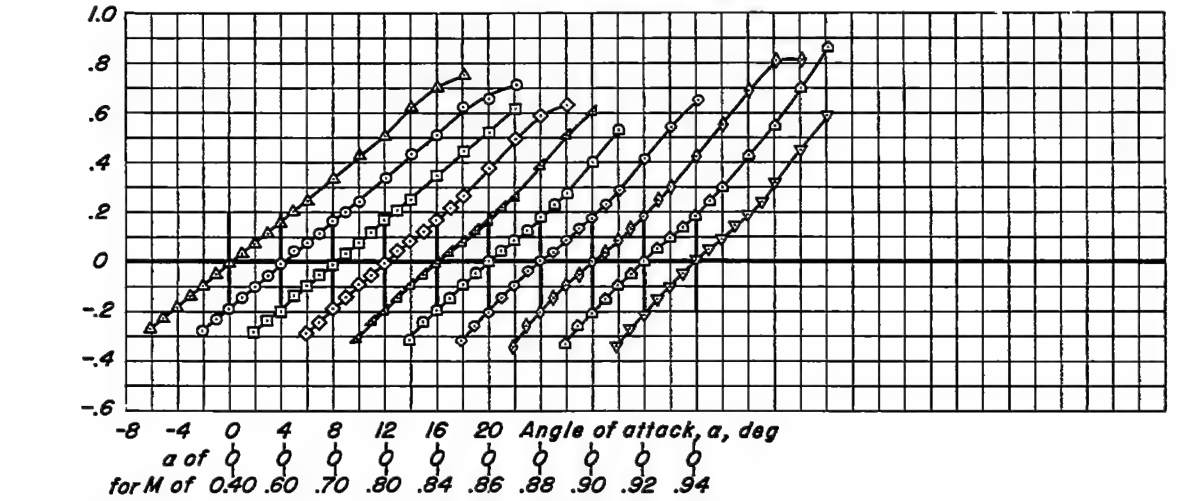

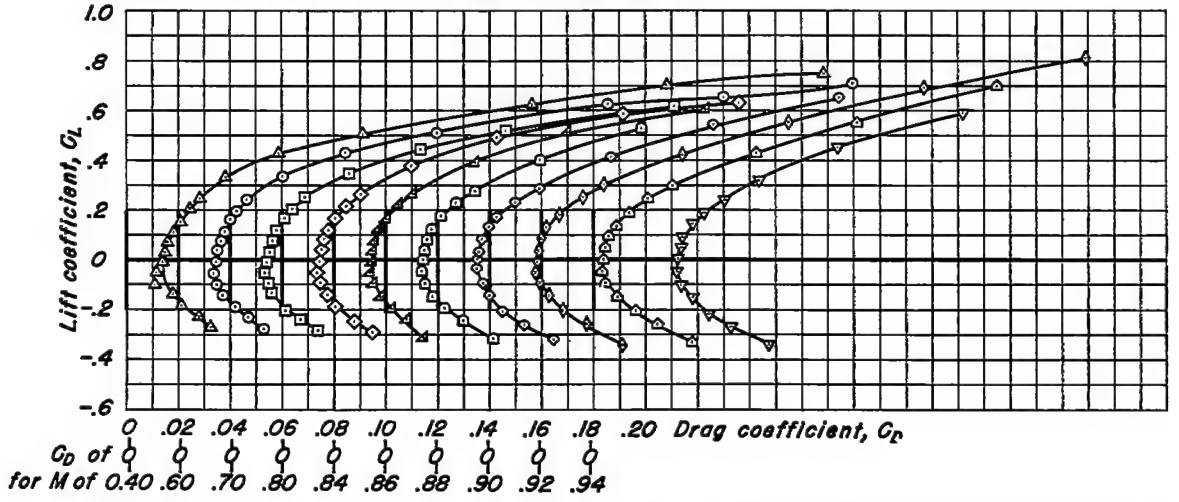

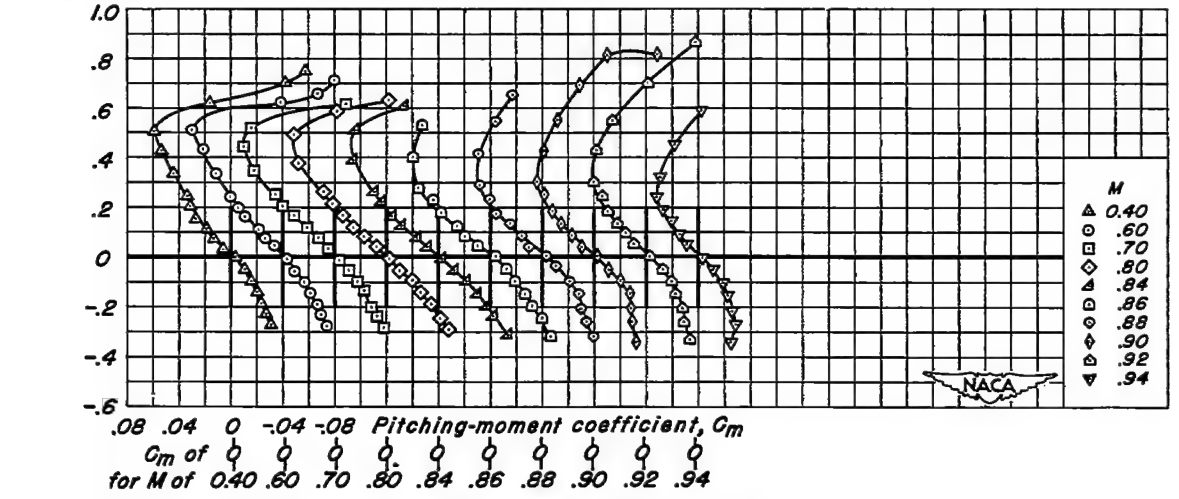

(b) Taper ratio 0.50.

Figure 12.- Concluded.

[redacted]

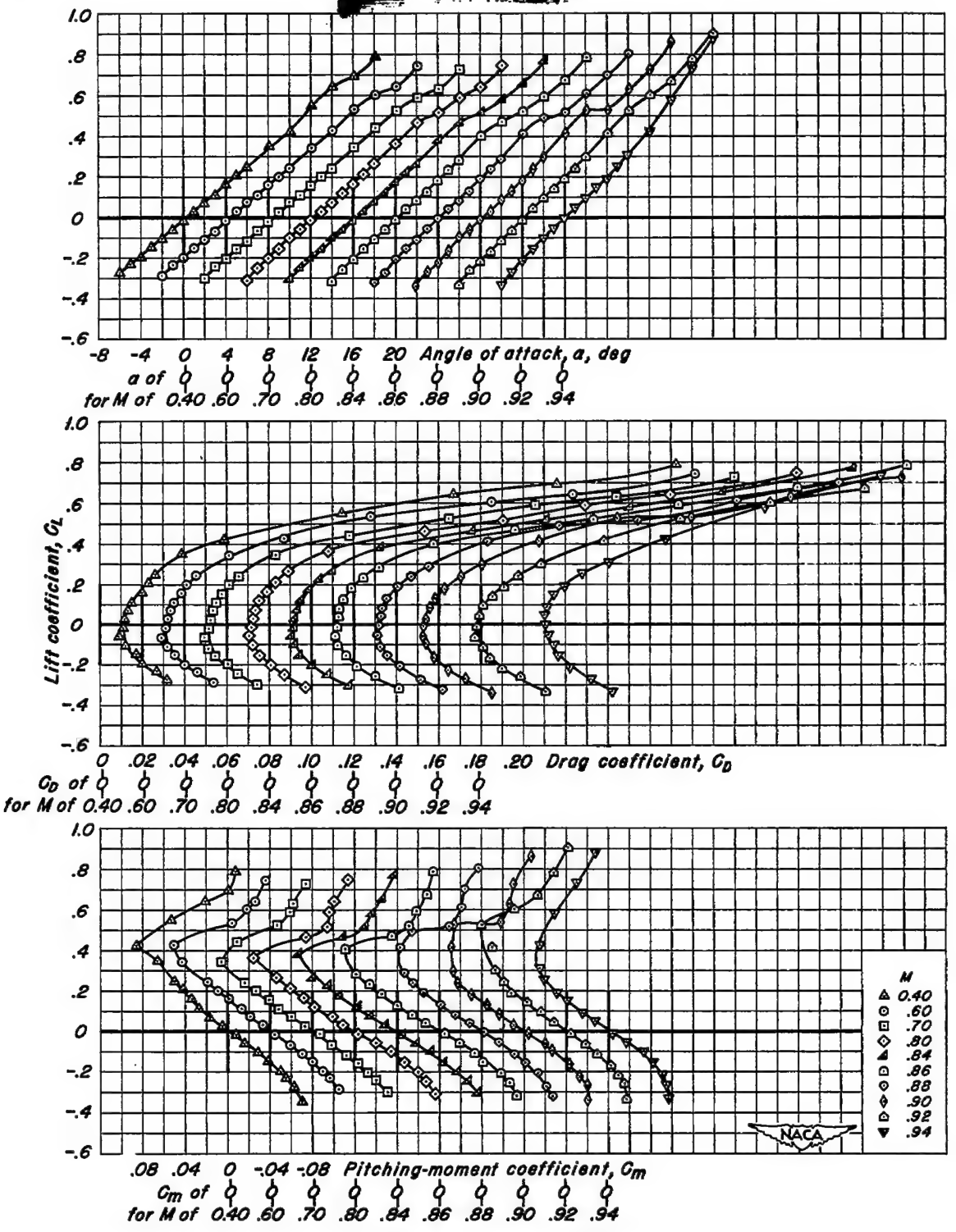

(a) Taper ratio 1.00.

Figure 13.- The lift, drag, and pitching-moment characteristics of the aspect ratio 2 wings in combination with the cylindrical body.

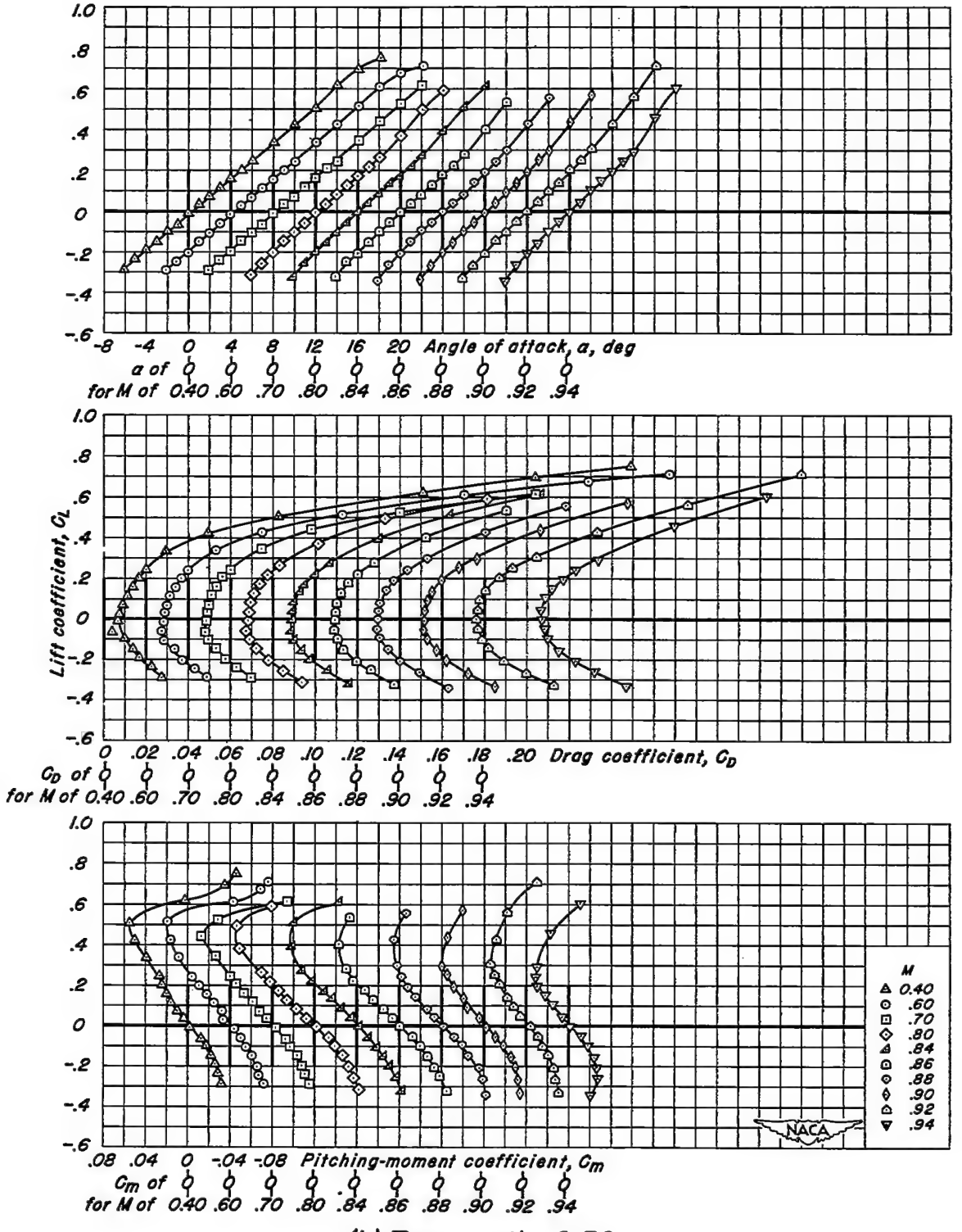

(b) Taper ratio 0.50.
Figure 13.- Concluded.

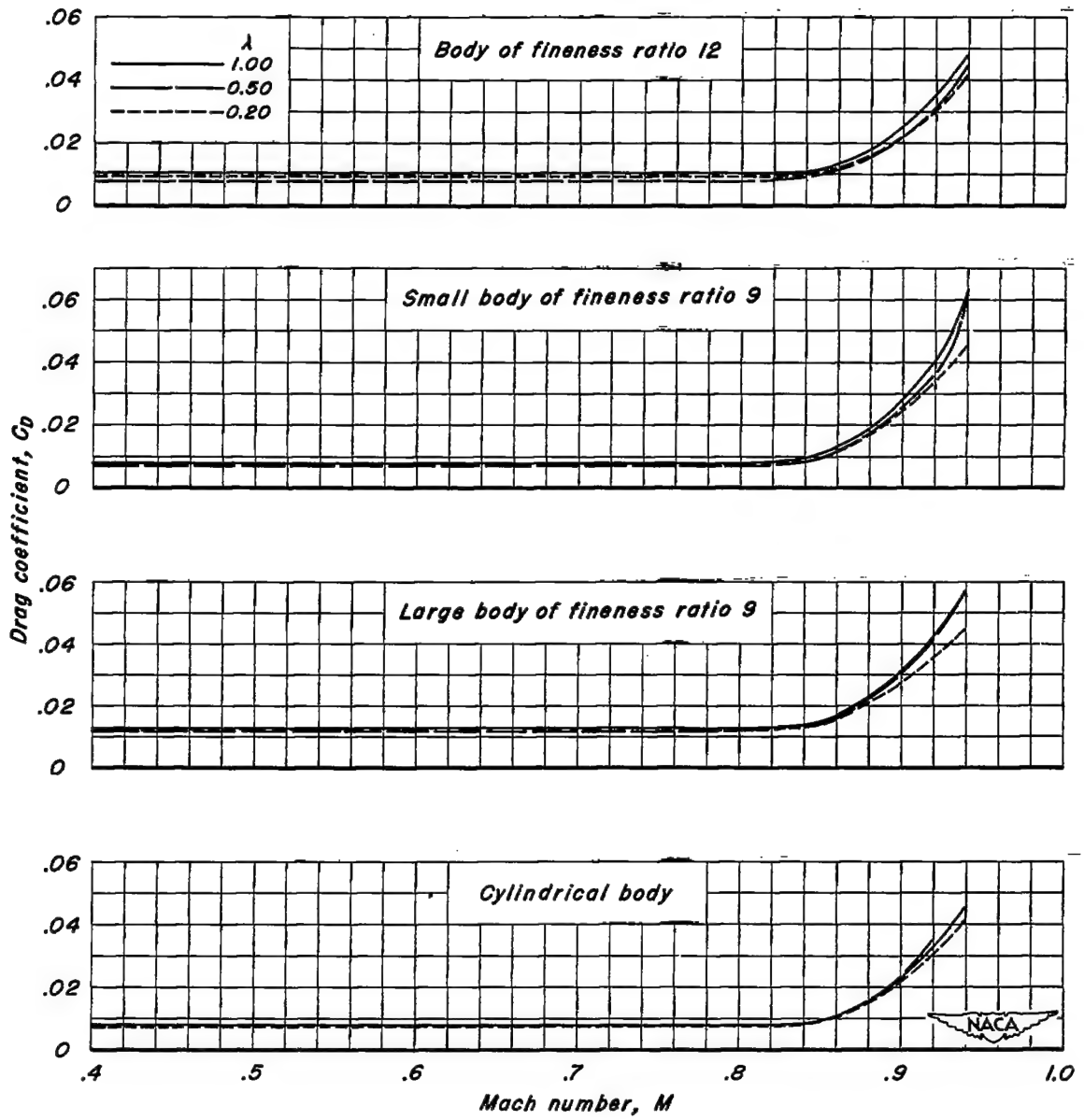

(a) Aspect ratio 4.

Figure 14.- The variation of drag coefficient, at zero lift, with Mach number for the wing-body combinations.

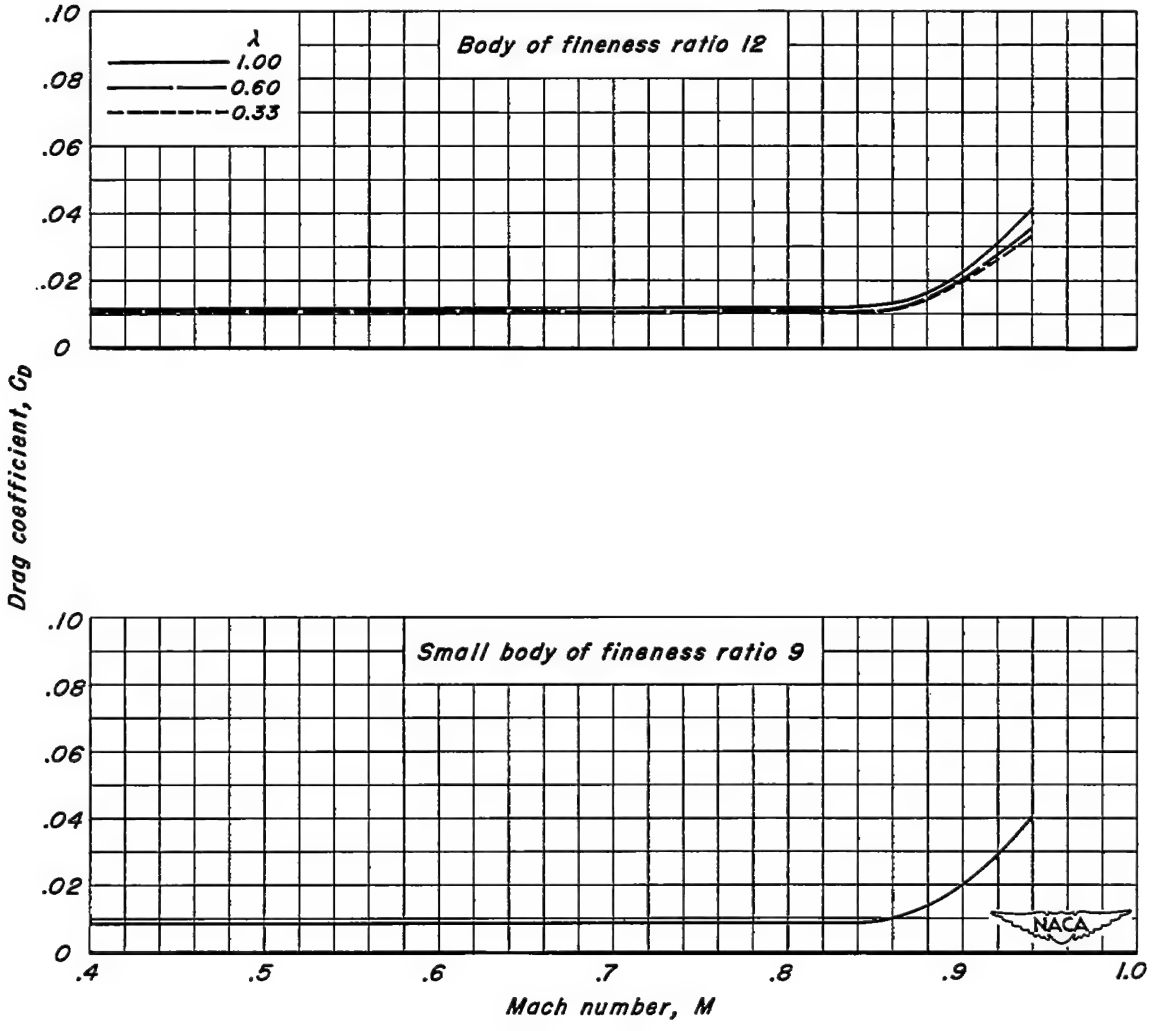

(b) Aspect ratio 3.
Figure 14.- Continued.

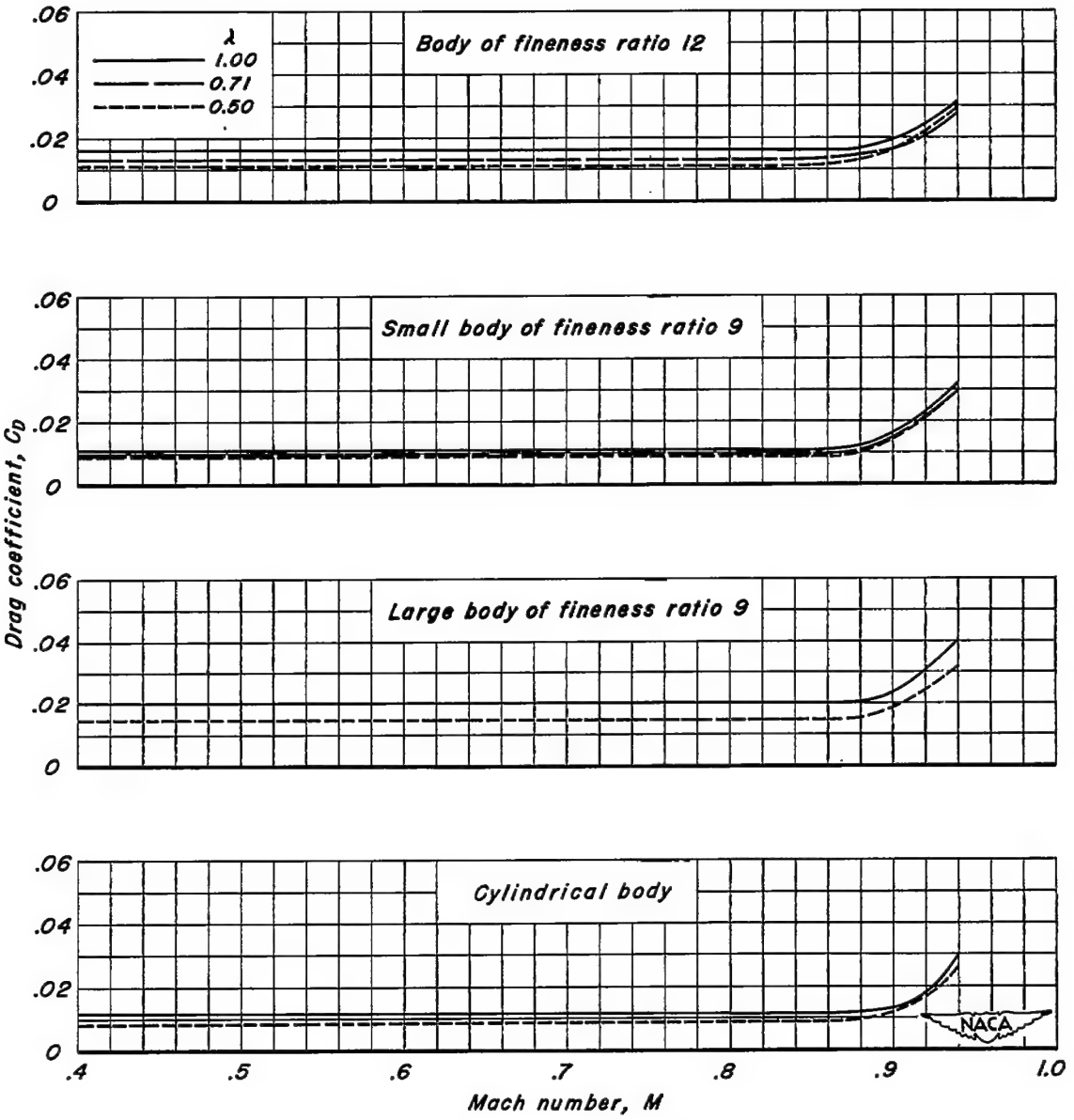

(c) Aspect ratio 2.
Figure 14.- Concluded.

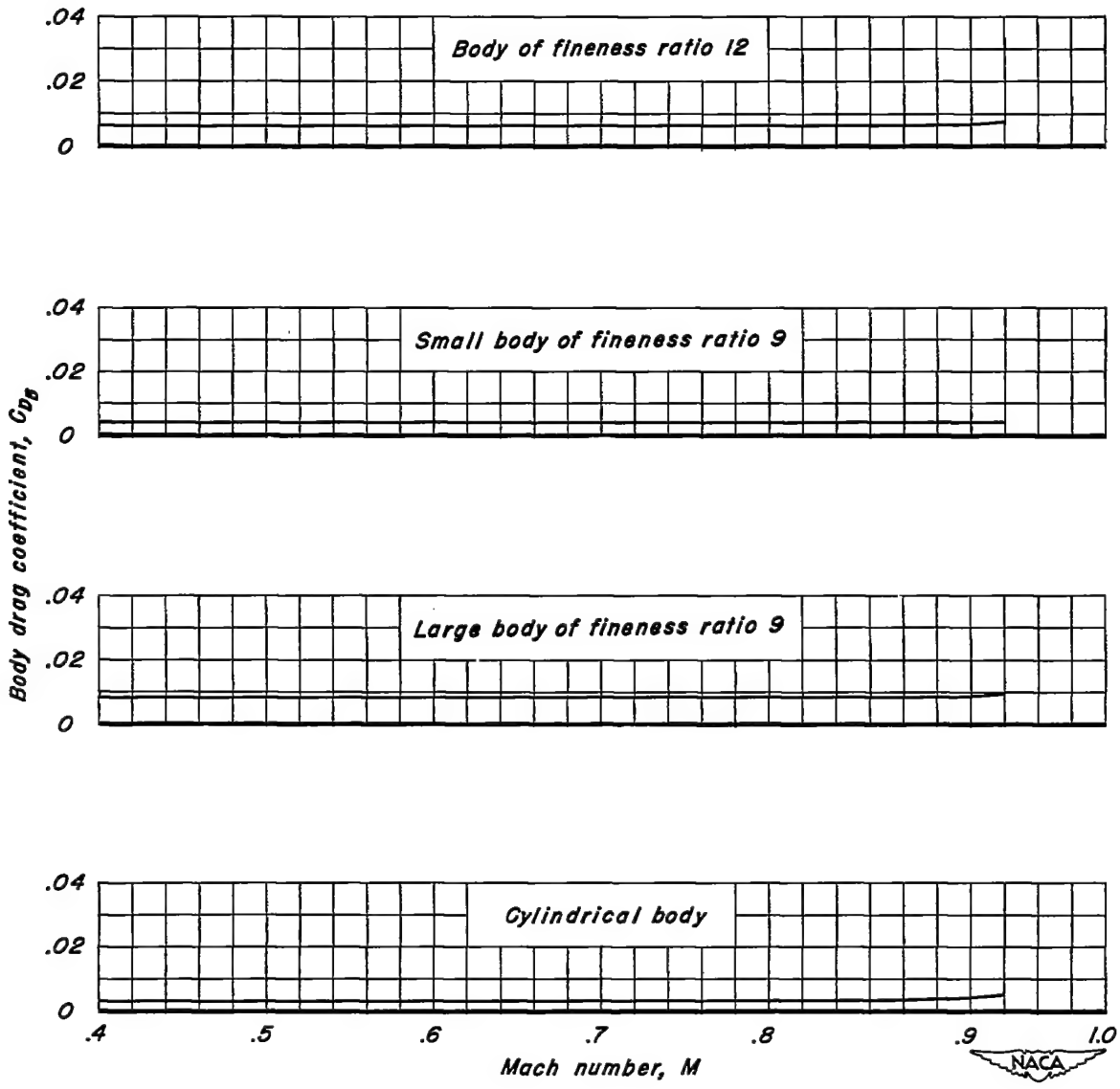

Figure 15.–The variation of minimum body drag coefficient with Mach number for the aspect ratio 4 wings.

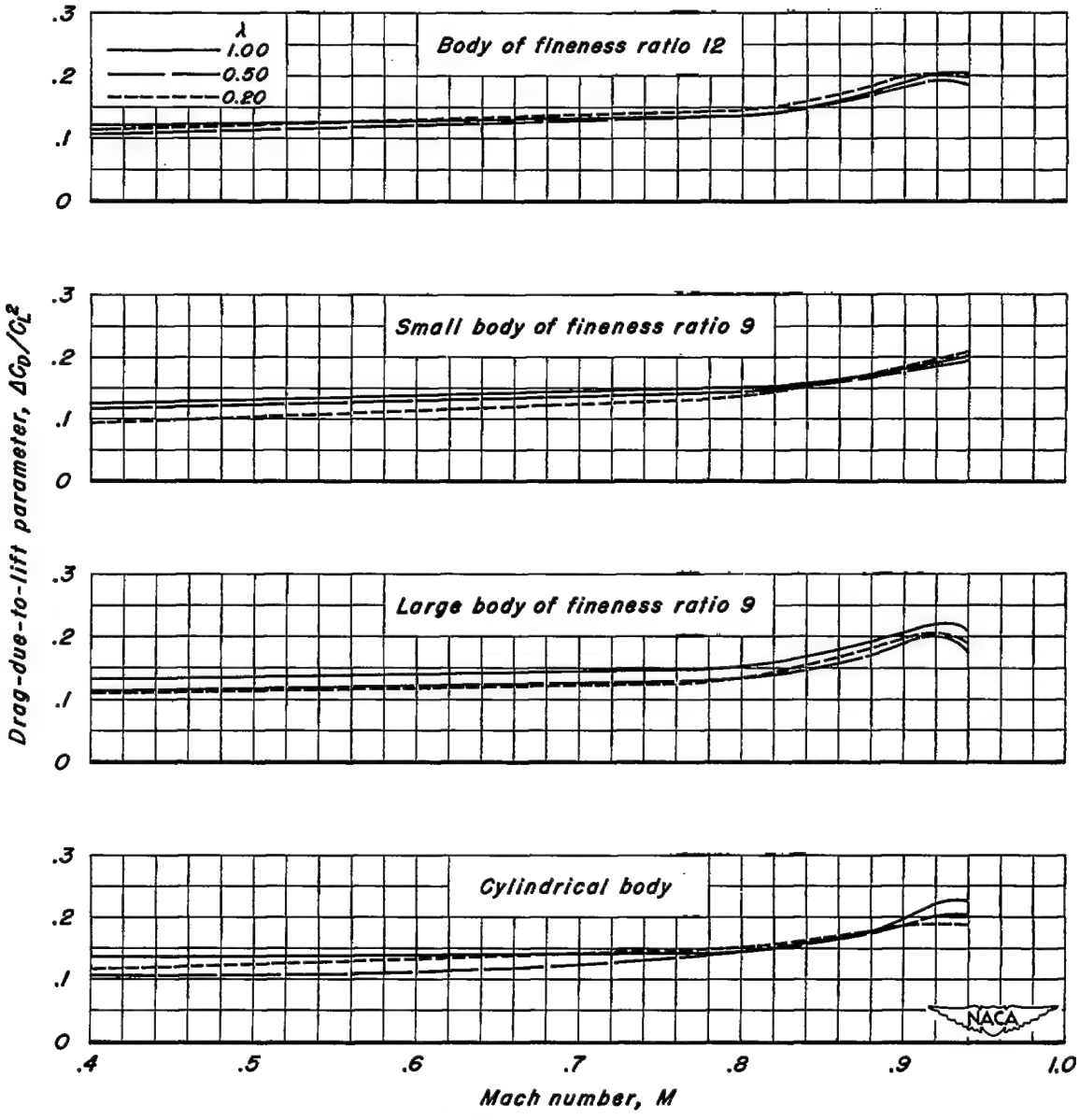

(a) Aspect ratio 4.

Figure 16.- The variation of drag due to lift parameter with Mach number.

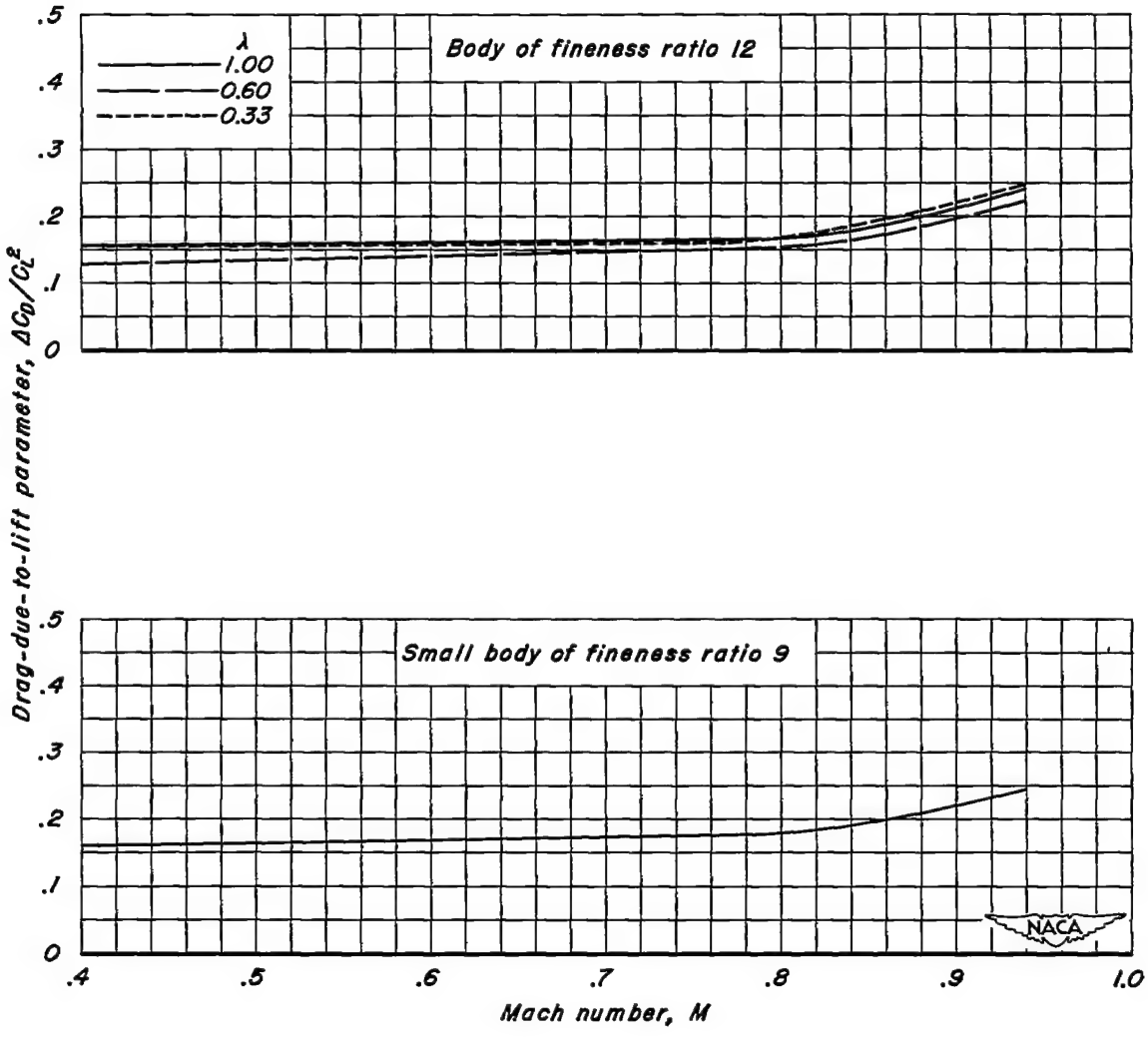

(b) Aspect ratio 3.
Figure 16.- Continued.

[redacted]

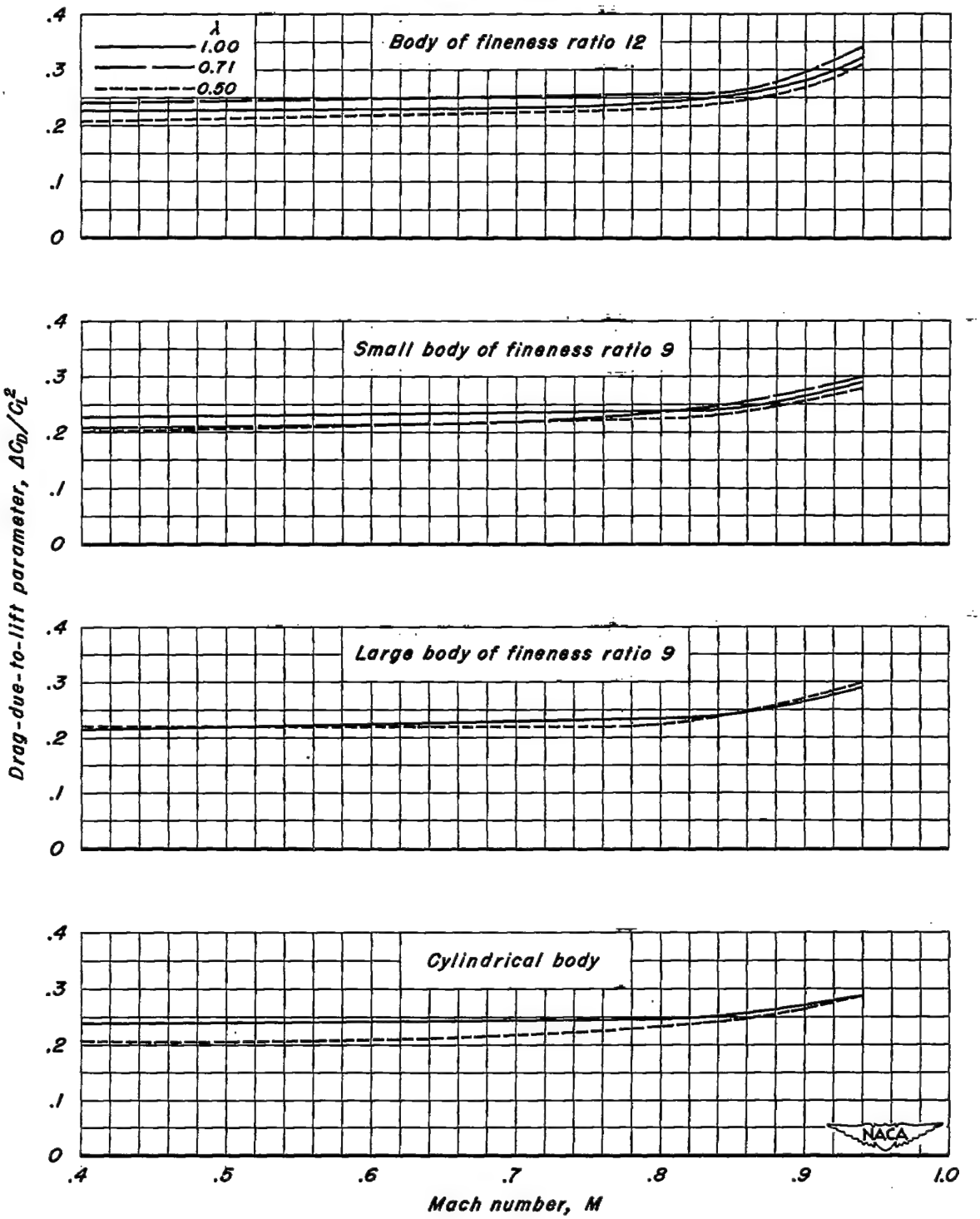

(c) Aspect ratio 2.
Figure 16.- Concluded.

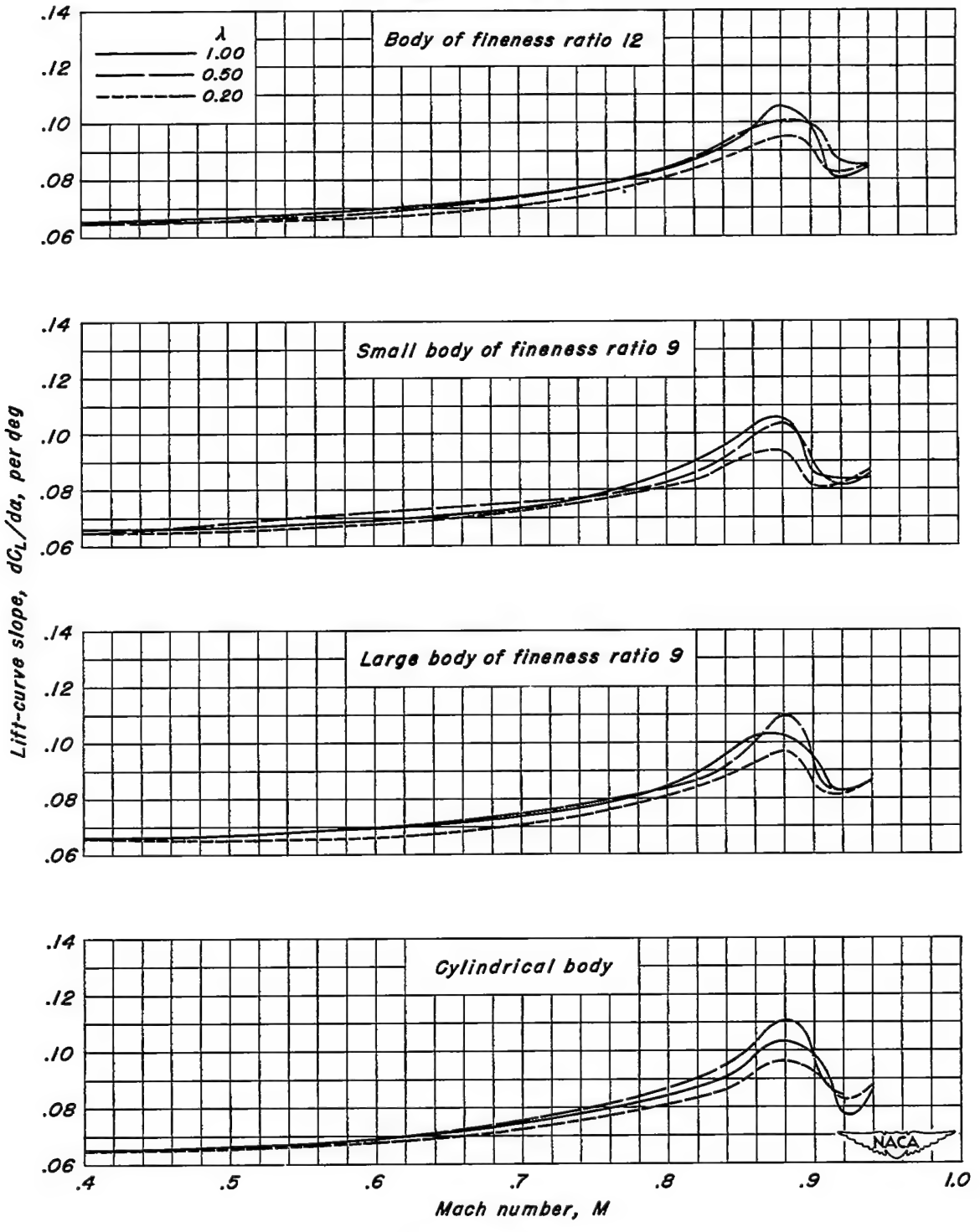

(a) Aspect ratio 4.

Figure 17.- The variation of lift-curve slope, at zero lift, with Mach number for the wing-body combinations.

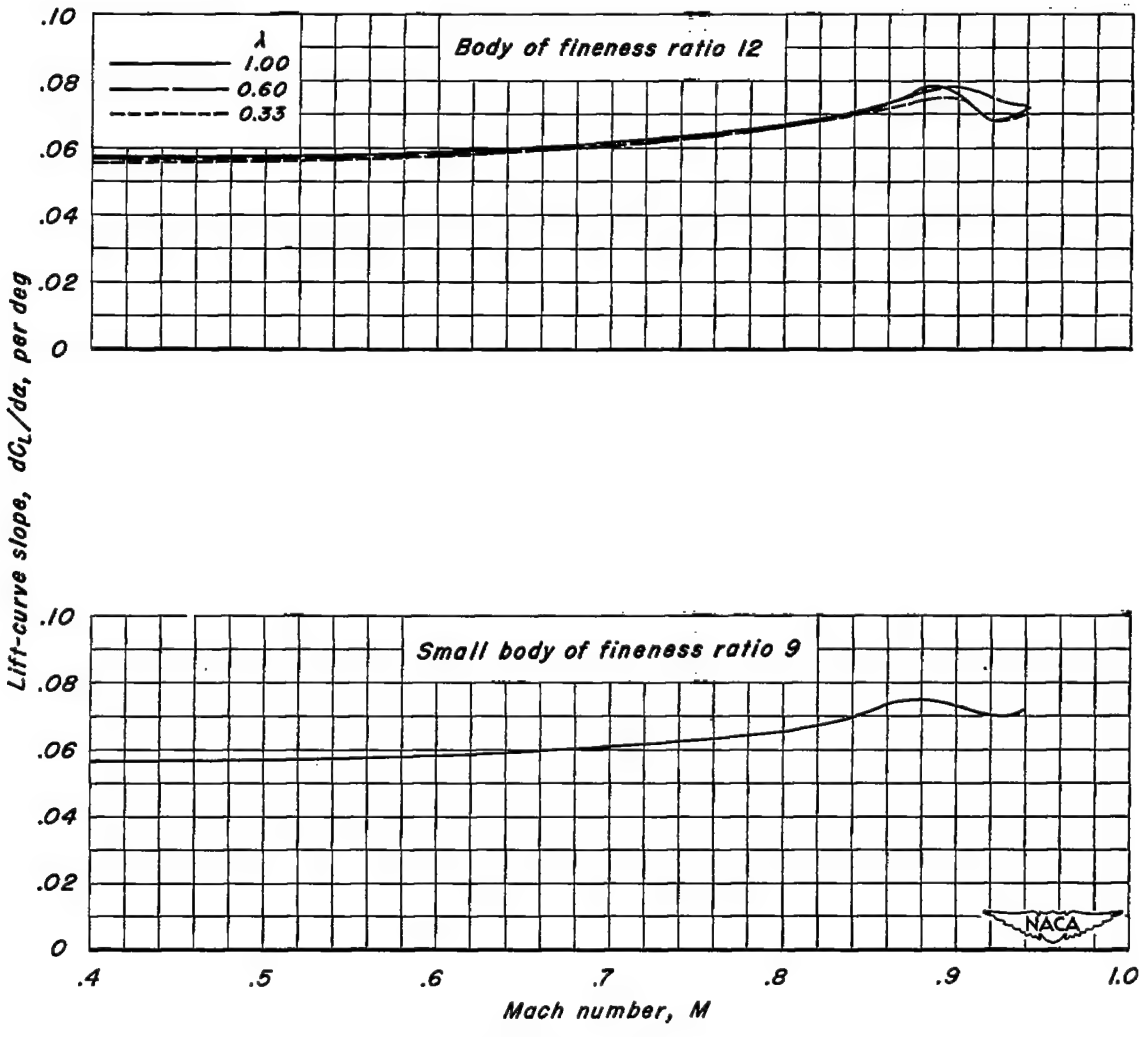

(b) Aspect ratio 3.
Figure 17.- Continued.

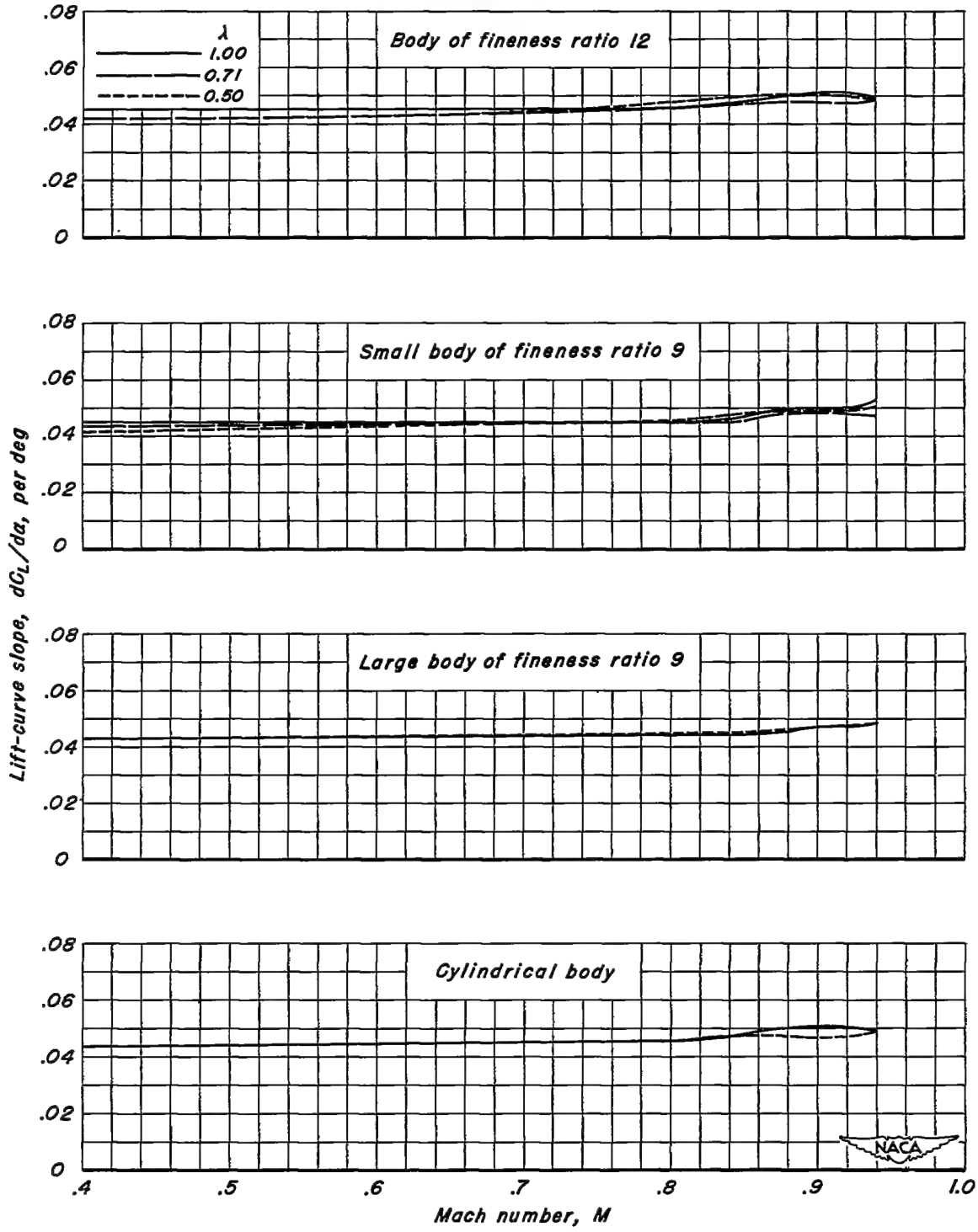

(c) Aspect ratio 2.
Figure 17.- Concluded.

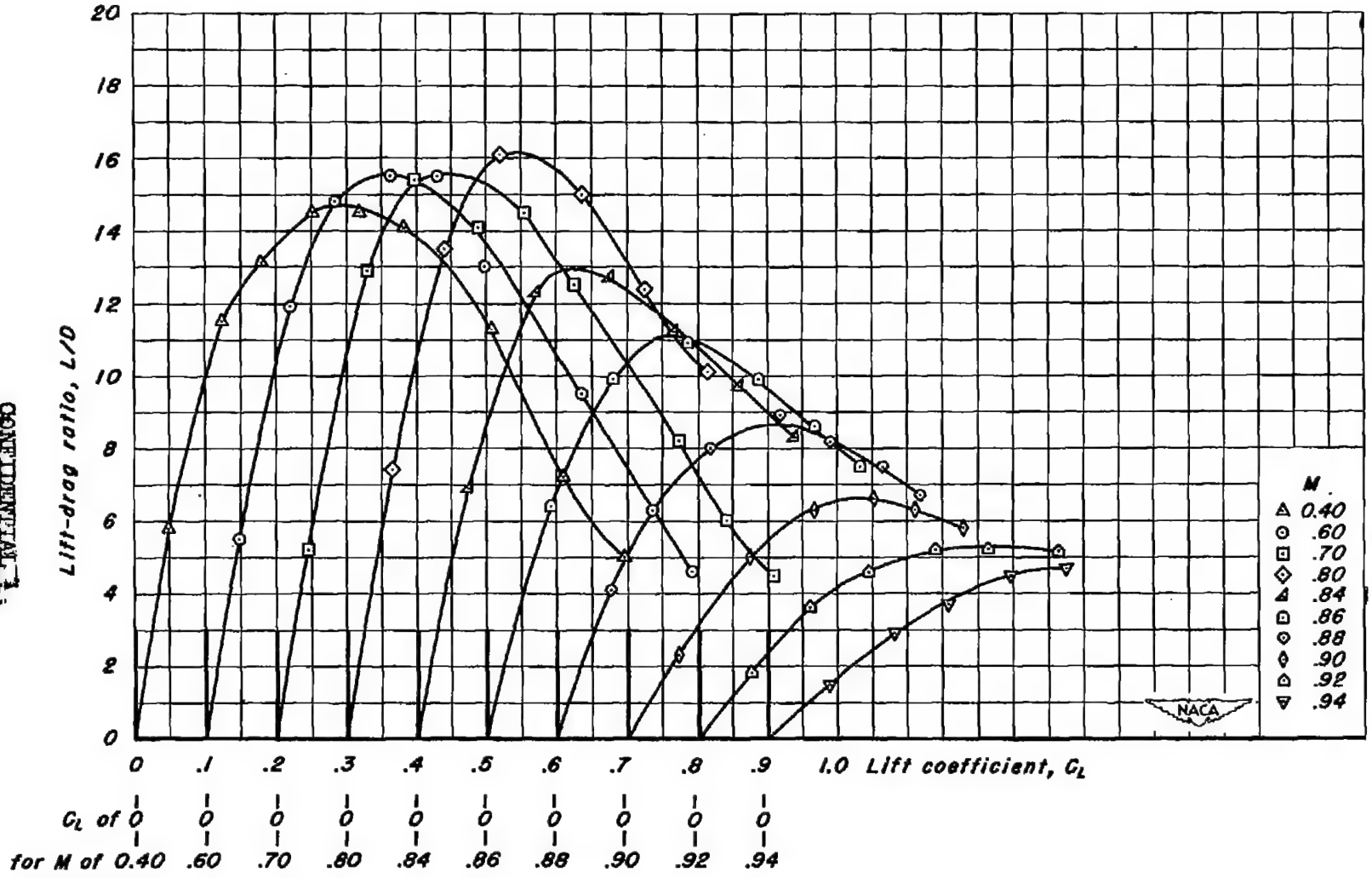

(a) Taper ratio 1.00.

Figure 18.- The variation of lift-drag ratio with lift coefficient of the aspect-ratio-4 wings in combination with the small body having a fineness ratio of 9.

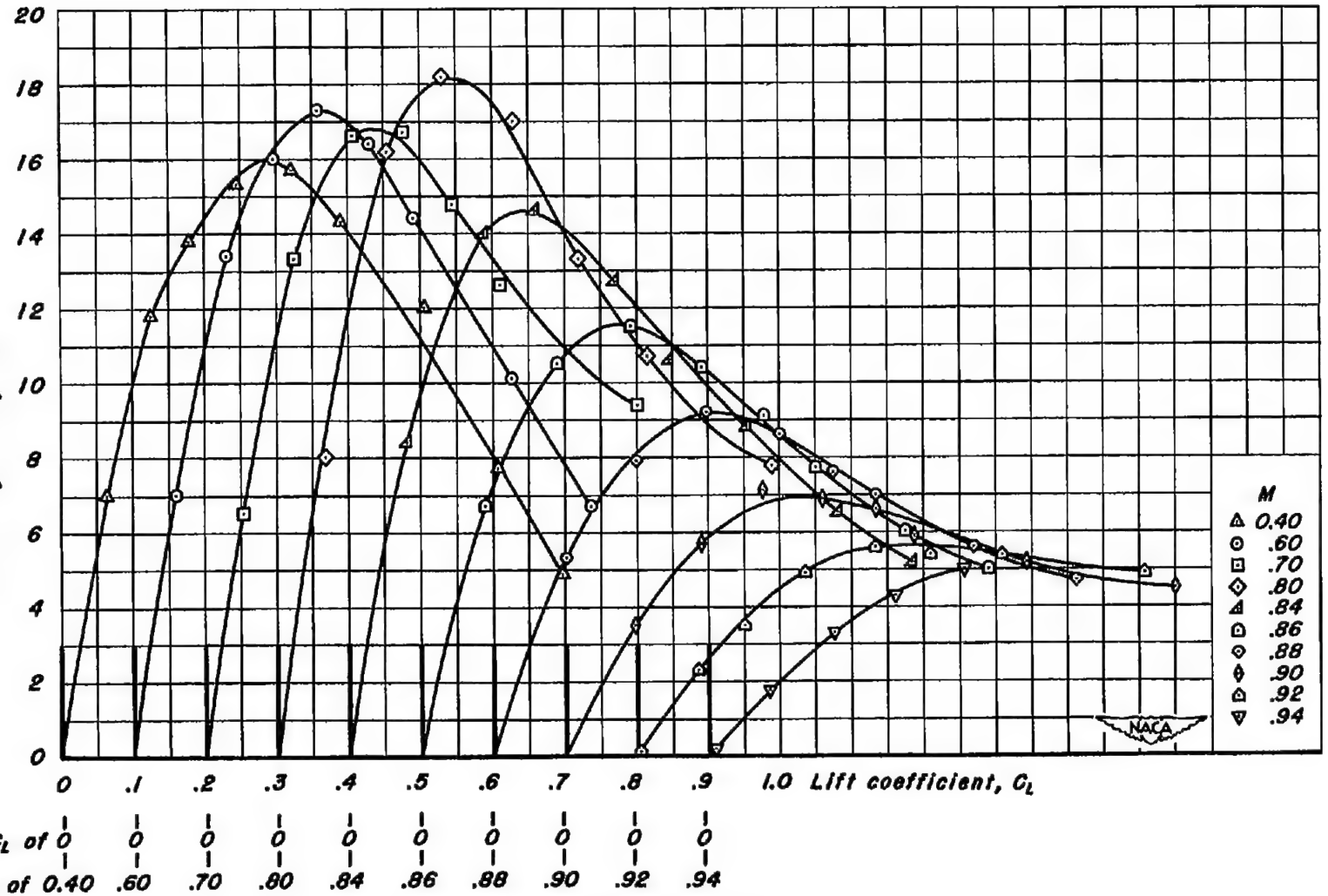

(b) Taper ratio 0.50.

Figure 18.- Continued.

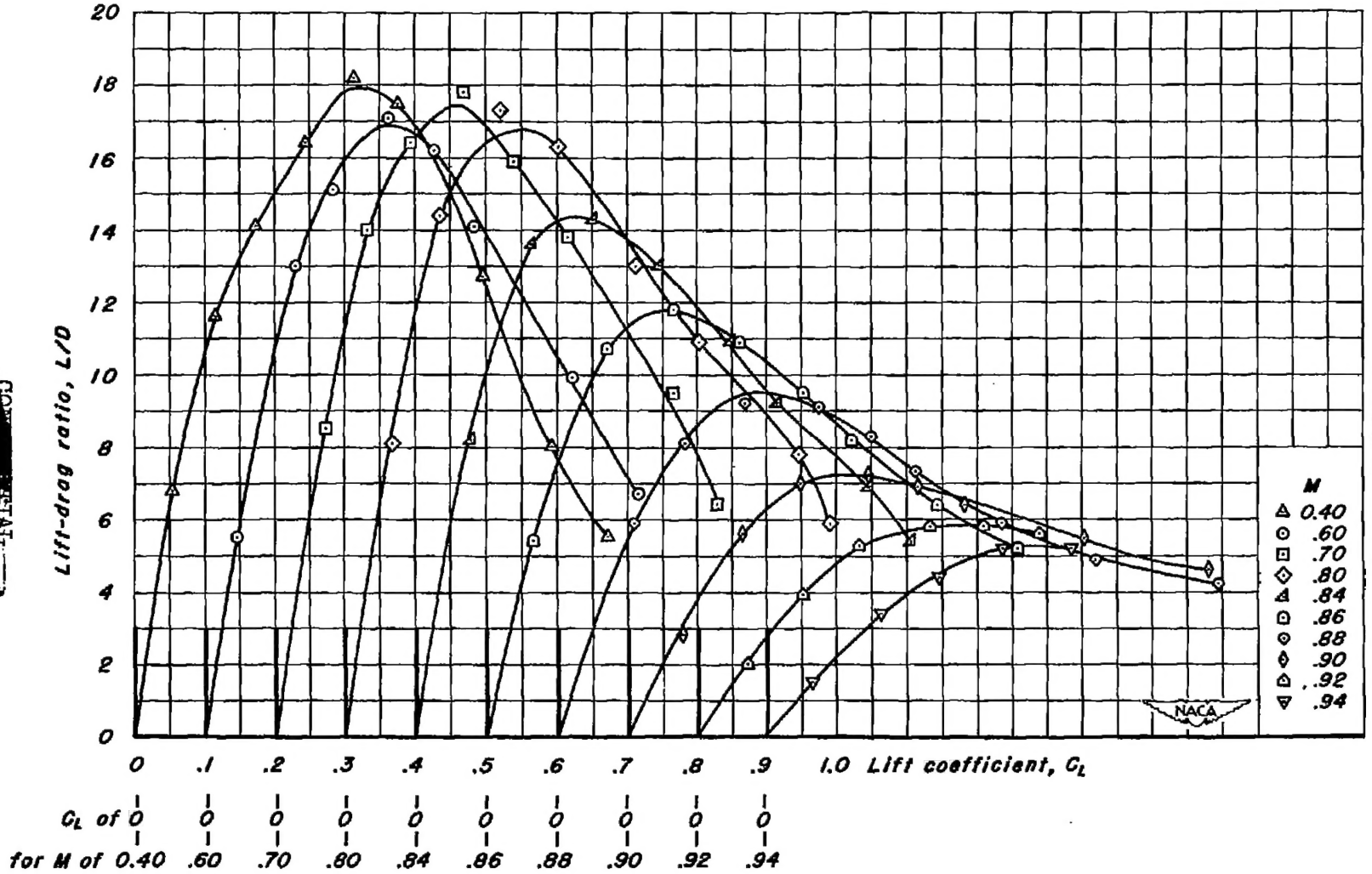

(c) Taper ratio 0.20.
Figure 18.- Concluded.

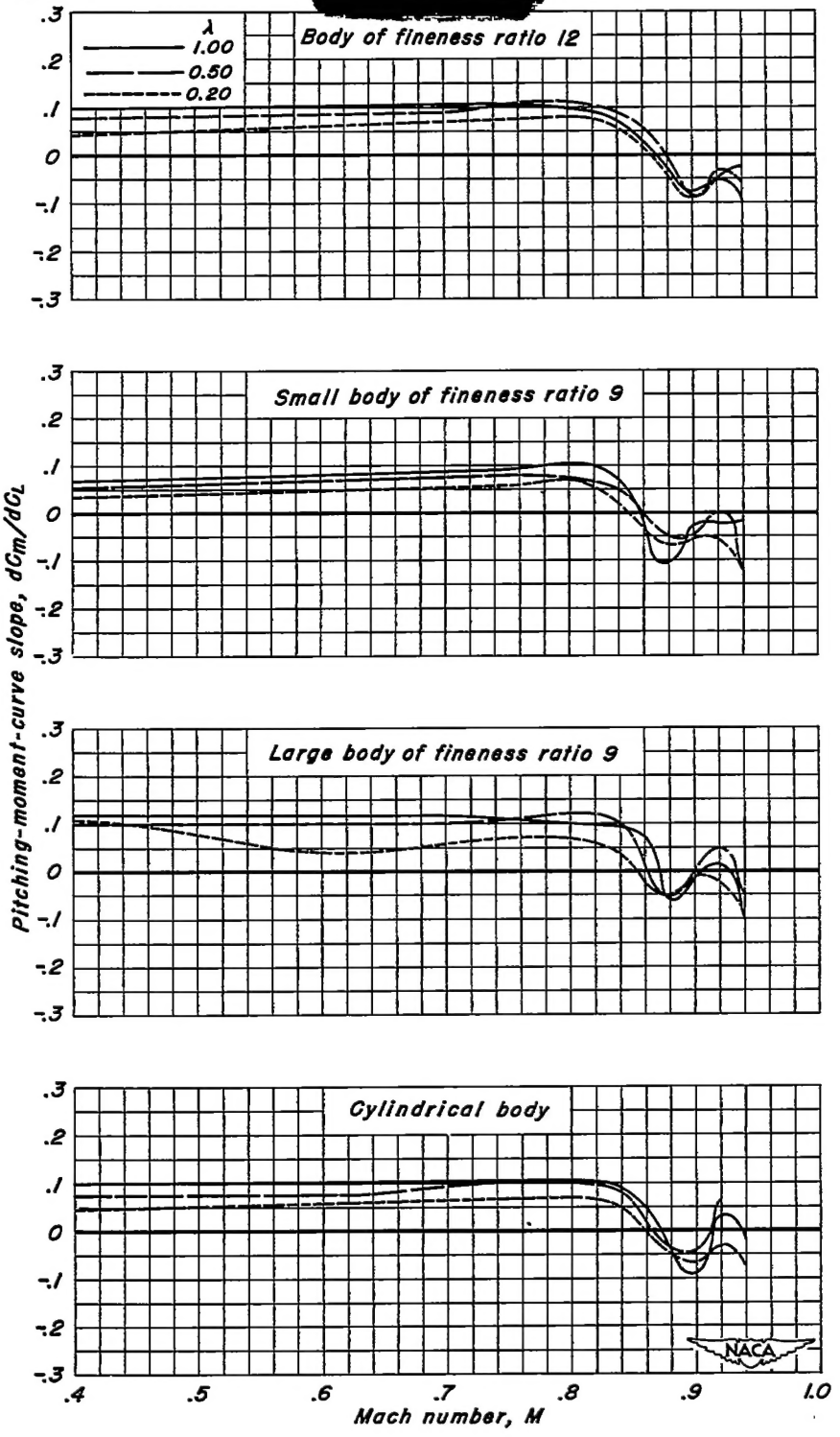

(a) Aspect ratio 4.

Figure 19.– The variation of pitching-moment-curve slope, at zero lift, with Mach number for the wing-body combinations.

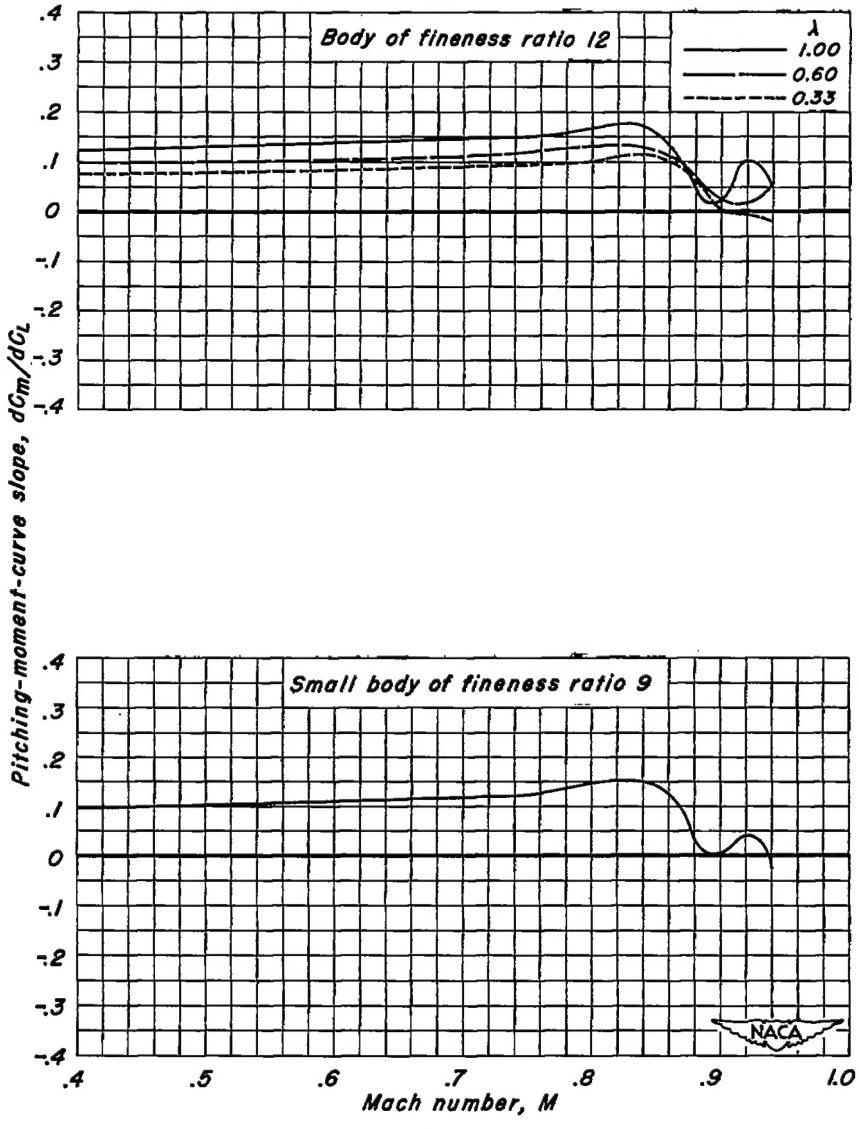

(b) Aspect ratio 3.
Figure 19.- Continued.

[redacted]

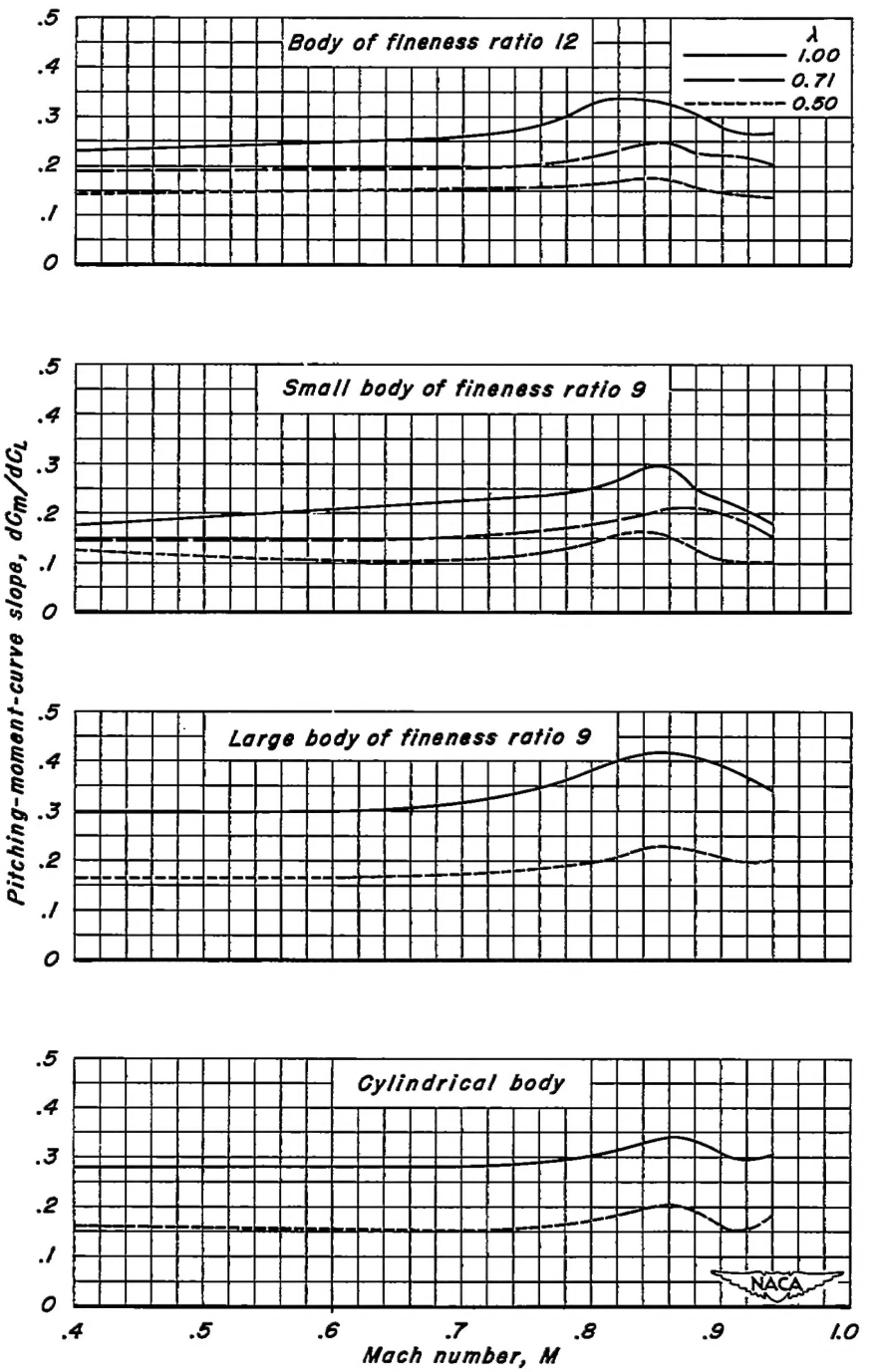

(c) Aspect ratio 2.
Figure 19.- Concluded.

[redacted]